Show me your secret(ed) weapons: a multifaceted approach reveals novel type III-secreted effectors of a plant pathogenic bacterium

Irene Jiménez Guerrero[1¶], Francisco Pérez-Montaño[1,2¶], Gustavo Mateus da Silva[1], Naama Wagner[3], Dafna Shkedy[3], Mei Zhao[4], Lorena Pizarro[5], Maya Bar[5], Ron Walcott[4], Guido Sessa[6], Tal Pupko[3], Saul Burdman[1]*

[1] Department of Plant Pathology and Microbiology, The Robert H. Smith Faculty of Agriculture, Food and Environment, The Hebrew University of Jerusalem, Rehovot, Israel

[2] Department of Microbiology, University of Seville, Seville, Spain

[3] The School of Molecular Cell Biology and Biotechnology, The George S. Wise Faculty of Life Sciences, Tel Aviv University, Tel Aviv, Israel

[4] Department of Plant Pathology, University of Georgia, Athens GA, USA

[5] Department of Plant Pathology and Weed Research, Agricultural Research Organization, The Volcani Center, Bet Dagan, Israel

[6] School of Plant Sciences and Food Security, The George S. Wise Faculty of Life Sciences, Tel Aviv University, Tel Aviv, Israel

*Corresponding author

E-mail: saul.burdman@mail.huji.ac.il

[¶]These authors contributed equally to this work.

Abstract

Many Gram-negative plant and animal pathogenic bacteria employ a type III secretion system (T3SS) to secrete protein effectors into the cells of their hosts and promote disease. The plant pathogen *Acidovorax citrulli* requires a functional T3SS for pathogenicity. As with *Xanthomonas* and *Ralstonia spp.*, an AraC-type transcriptional regulator, HrpX, regulates expression of genes encoding T3SS components and type III-secreted effectors (T3Es) in *A. citrulli.* A previous study reported eleven T3E genes in this pathogen, based on the annotation of a sequenced strain. We hypothesized that this was an underestimation. Guided by this hypothesis, we aimed at uncovering the T3E arsenal of the *A. citrulli* model strain, M6. We carried out a thorough sequence analysis searching for similarity to known T3Es from other bacteria. This analysis revealed 51 *A. citrulli* genes whose products are similar to known T3Es. Further, we combined machine learning and transcriptomics to identify novel T3Es. The machine learning approach ranked all *A. citrulli* M6 genes according to their propensity to encode T3Es. RNA-Seq revealed differential gene expression between wild-type M6 and a mutant defective in HrpX. Data combined from these approaches led to the identification of seven novel T3E candidates, that were further validated using a T3SS-dependent translocation assay. These T3E genes encode hypothetical proteins, do not show any similarity to known effectors from other bacteria, and seem to be restricted to plant pathogenic *Acidovorax* species. Transient expression in *Nicotiana benthamiana* revealed that two of these T3Es localize to the cell nucleus and one interacts with the endoplasmic reticulum. This study not only uncovered the arsenal of T3Es of an important pathogen, but it also places *A. citrulli* among the "richest" bacterial pathogens in terms of T3E cargo. It also revealed novel T3Es that appear to be involved in the pathoadaptive evolution of plant pathogenic *Acidovorax* species.

Author summary

Acidovorax citrulli is a Gram-negative bacterium that causes bacterial fruit blotch (BFB) disease of cucurbits. This disease represents a serious threat to cucurbit crop production worldwide. Despite the agricultural importance of BFB, the knowledge about basic aspects of *A. citrulli*-plant interactions is rather limited. As many Gram-negative plant and animal pathogenic bacteria, *A. citrulli* employs a complex secretion system, named type III secretion system, to deliver protein virulence effectors into the host cells. In this work we aimed at uncovering the arsenal of type III-secreted effectors (T3Es) of this pathogen by combination of bioinformatics and experimental approaches. We found that this bacterium possesses at least 51 genes that are similar to T3E genes from other pathogenic bacteria. In addition, our study revealed seven novel T3Es that seem to occur only in *A. citrulli* strains and in other plant pathogenic *Acidovorax* species. We found that two of these T3Es localize to the plant cell nucleus while one partially interacts with the endoplasmic reticulum. Further characterization of the novel T3Es identified in this study may uncover new host targets of pathogen effectors and new mechanisms by which pathogenic bacteria manipulate their hosts.

Introduction

The genus *Acidovorax* (class Betaproteobacteria) contains a variety of species with different lifestyles. While some species are well adapted to soil and water environments, others have developed intimate relationships with eukaryotic organisms, including as plant pathogens [1]. Among the latter, *Acidovorax citrulli* is one of the most important plant pathogenic species [2]. This bacterium infects all aerial parts of cucurbit plants, causing bacterial fruit blotch (BFB) disease. The unavailability of effective tools for managing BFB, including the lack of resistance sources, and the disease's high destructive potential, exacerbate the threat BFB poses to cucurbit (mainly melon and watermelon) production [3, 4]. Despite the economic importance of BFB, little is known about basic aspects of *A. citrulli*-plant interactions.

On the basis of genetic and biochemical features, *A. citrulli* strains are divided into two main groups: group I strains have been generally isolated from melon and other non-watermelon cucurbits, whereas group II strains have been mainly isolated from watermelon [5-7]. *Acidovorax citrulli* M6 is a group I strain that was isolated in 2002 from a BFB outbreak of melons in Israel [5], and subsequently became a model group I strain for investigation of basic aspects of BFB. The *A. citrulli* M6 genome has been sequenced, first by Illumina MiSeq [8] and recently, by PacBio [9], which allowed its complete closure.

As many Gram-negative plant and animal pathogenic bacteria, *A. citrulli* relies on a functional type III secretion system (T3SS) to promote disease [10]. This complex secretion system is employed by these pathogens to deliver protein effectors into target eukaryotic cells. Collectively, type III-secreted effectors (T3Es) promote disease by modulating a variety of cellular functions for the benefit of the pathogen [11-13]. In the case of plant pathogenic bacteria, type III-secreted effectors (T3Es) were shown to

promote virulence through alteration of the plant cell metabolism and/or suppression of host immune responses [14, 15]. As part of their defence mechanism, plants recognize some effectors by corresponding disease resistance (R) proteins, mostly belonging to the nucleotide-binding (NB)-leucine-rich repeat (LRR) type of immune receptors (NLRs) [16, 17]. Upon effector recognition, the R protein elicits a battery of defense responses collectively referred to as effector-triggered immunity (ETI). ETI is often accompanied by the hypersensitive response (HR), a rapid death of plant cells at the infection site that arrests pathogen spread in the plant tissue [18]. Therefore, elucidating the arsenal of effectors and their contribution to virulence, are of critical importance for the understanding of basic aspects of pathogenicity but also for translational research in the crop protection field.

Due to the requirement of type III secretion (T3S) for pathogenicity in susceptible plants and HR elicitation in resistant plants, the genes encoding key T3SS regulators and structural components in plant pathogenic bacteria are named *hrp* genes (for HR and pathogenicity) or *hrc* genes, in the case of *hrp* genes that are conserved among different bacterial genera, including in animal pathogens [19]. On the basis of gene content, operon organization and regulation, *hrp* clusters are divided into two classes: class I contains the *hrp* clusters of *Pseudomonas syringae* and enteric plant pathogenic bacteria, while class II contains the clusters of *Xanthomonas* species, *Ralstonia solanacearum* and plant pathogenic *Acidovorax* spp. [10, 19, 20] .

In *Xanthomonas* spp. and *R. solanacearum*, the expression of *hrp*, *hrc* and *hrp*-associated (*hpa*) genes, as well as of some T3E genes, is regulated by HrpG and HrpX/HrpB (HrpX in *Xanthomonas* spp. and HrpB in *R. solanacearum*). HrpG belongs to the OmpR family of two-component system response regulators and controls expression of *hrpX*/*hrpB* [21-23]. *hrpX* and *hrpB* encode AraC-type transcriptional

activators that directly mediate the expression of most *hrp*/*hrc* operons and many T3E genes, via binding to DNA motifs that are present in their promoter regions. These DNA motifs are named plant-inducible promoter (PIP) box (TTCGB-N15-TTCGB; B being any nucleotide except adenine) in *Xanthomonas* spp. [24] and hrp_{II} box (TTCG-N16_TTCG) in *R. solanacearum* [25]. Recently, Zhang *et al.* showed that the *hrpG* and *hrpX*/*hrpB* (thereafter *hrpX*) orthologous genes of the *A. citrulli* group II strain Aac5 are required for pathogenicity [26]. They also showed that HrpG activates expression of *hrpX*, which in turn, regulates the expression of a T3E gene belonging to the YopJ family.

Until recently, based on the annotation of the genome of the *A. citrulli* group II strain AAC00-1, we were aware of eleven genes showing similarity to known T3E genes from other bacteria [27]. Considering the higher numbers of T3E genes in several other plant pathogenic bacteria, we hypothesized that this is an underestimation of the actual number of T3Es in *A. citrulli*. We also hypothesized that *A. citrulli* may carry novel T3E genes that were not previously described in other bacteria. Guided by these hypotheses, we carried out a detailed sequence analysis of *A. citrulli* M6 open reading frames (ORFs) to identify genes with similarity to known T3E genes from other bacteria. We also combined machine-learning (ML) and RNA-Seq approaches to identify putative, novel *A. citrulli* T3Es. Further, we adapted a T3E translocation assay to verify T3S-dependent translocation of candidate effectors. Combining these approaches allowed identification of seven new T3Es that appear to be unique to plant pathogenic *Acidovorax* species. Subcellular localization of three of these T3Es in *N. benthamiana* leaves was also determined by *Agrobacterium*-mediated transient expression.

Results

Identification of new T3E genes of *A. citrulli* by genome annotation, machine learning and sequence analyses

Analysis of the genome of the group II *A. citrulli* strain AAC00-1 (GenBank accession CP000512.1) revealed eleven genes similar to T3E genes of other plant pathogenic bacteria [27]. These genes were present in all tested group II strains. In contrast, all assessed group I strains, including M6, lacked the effector gene *Aave_2708* (gene ID according to the AAC00-1 annotation), encoding a *Xanthomonas euvesicatoria* XopJ homolog. Group I strains also had disrupted open reading frames (ORFs) in the genes *Aave_3062*, encoding an effector similar to *Xanthomonas oryzae* pv. *oryzicola* AvrRxo1, and *Aave_2166*, encoding a *X. euvesicatoria* AvrBsT homolog [27].

To identify new putative T3E genes of *A. citrulli* we applied a machine learning (ML) approach, that was successfully utilized for identification of new T3E genes of *X. euvesicatoria* [28] and *Pantoea agglomerans* [29]. Using this algorithm, all ORFs of a bacterial genome are scored according to their propensity to encode T3Es. The scoring is based on a large set of features including similarity to known T3E genes, genomic organization, amino acid composition bias, characteristics of the putative N-terminal translocation signal and GC content, among others (see Methods).

An initial ML run was used to classify all ORFs of strain AAC00-1 according to their probability to encode T3Es. This strain, rather than M6, was used for learning and prediction, because at the time this ML was conducted, the AAC00-1 genome was fully assembled with better annotation. For training, the positive set included 12 AAC00-1 genes that encoded T3E homologs: the eleven genes described by Eckshtain-Levi *et al.* [27] and one additional gene, *Aave_2938* that is identical to *Aave_2708*. The negative

set included genes that showed high sequence similarity to ORFs of a non-pathogenic *Escherichia coli* strain. The output of this ML run was a list of all annotated genes of *A. citrulli* AAC00-1 ranked by their propensity to encode T3Es (S1 Table). For each ORF, we searched for the homolog in *A. citrulli* M6. Among the top predictions from AAC00-1, many genes did not have homologs in M6. As expected, the aforementioned 12 positive T3E genes of AAC00-1 were ranked high in this list (among the 36 highest scoring predictions, with eight being ranked among the top 10, and eleven among the top 15; S1 Table). Results from this first ML run served, together with RNA-Seq data, as the basis for selection of candidate T3E (CT3E) genes for experimental validation (see below).

In parallel, we performed an extensive homology search, using BlastP, to identify additional putative T3E genes of *A. citrulli* M6. This analysis led to the identification of many additional genes with significant similarity to T3E genes from other plant pathogenic bacteria. Table 1 summarizes the arsenal of putative T3E genes of *A. citrulli* M6, based on its genome annotation and sequence similarity analysis. Overall, we found 51 putative T3E genes in the *A. citrulli* M6 genome, in support of the notion that *A. citrulli* has a larger T3E repertoire than previously estimated. Most of these genes also received high scores in the ML search ranking among the top 100 ORFs (Table 1 and S1 Table). With that said, ten genes encoding T3E homologs were ranked in very low positions in the ML run (positions 231 to 1161; Table 1). On the other hand, many top ranked genes were annotated as encoding hypothetical proteins, some of which could encode yet unknown T3Es.

Table 1. List of putative T3E genes of *Acidovorax citrulli* M6 based on genome annotation and sequence similarity (BlastP) to known T3E genes from other plant pathogenic bacteria.

Locus_tag M6[1]	Annotation in M6[1]	Similarity[2]	ML1[3]	ML2[3]	Locus_tag AAC00-1[4]	X[5]	R[5]	P[5]
APS58_0030	*HP*	Type III effector HopBN1	171	8	*Aave_2531*	+	+	+
APS58_0167[6]	*avrBsT*	Avirulence protein AvrBsT	3	15	*Aave_2166*	+	+	+
APS58_0178	*HP*	Type III effector HopF2	not in ML1	131	-	+	(+)	+
APS58_0492	*avrPphE*	Avirulence protein AvrPphE family	14	32	*Aave_3452*	+	+	+
APS58_0502	*yopJ*	Type III effector YopP/ AvrRxv family	5	23	*Aave_3462*	+	+	(+)
APS58_0506	*HP*	Avirulence protein AvrPphE family	not in ML1	12	-	+	+	+
APS58_0542	*hopD2*	Type III effector HopD2/HopAO1	28	26	*Aave_3502*	+	+	+
APS58_0658	*HP*	Type III effector XopN	103	13	*Aave_3621*	+	+	+
APS58_0664	*HP*	Type III effector XopQ	86	107	*Aave_3626*	+	+	+
APS58_0885	*HP*	Type III effector (*R. solanacearum*)	231	81	*Aave_3847*	(+)	+	-
APS58_1000	*HP*	Type III effector protein	814	98	*Aave_3961*	+	+	-
APS58_1023	*xopD*	Type III effector XopD	265	38	*Aave_4359*	+	(+)	(+)
APS58_1209	*HP*	Type III effector YopP/ AvrRxv family	not in ML1	3	-	-	+	-
APS58_1255	*HP*	Type III effector XopAE	161	18	*Aave_4254*	+	-	-
APS58_1433	*HP*	Type III effector HopBD1	367	42	*Aave_4427*	+	-	+
APS58_1482	*HP*	Type III effector XopF1	241	28	*Aave_4472*	+	-	(+)
APS58_1627	*HP*	Type III effector protein	223	143	*Aave_4606*	-	+	-
APS58_1634	*HP*	Type III effector XopR	51	24	*Aave_4612*	+	-	-
APS58_1657	*HP*	LRR protein, type III effector PopP	73	110	*Aave_4631*	+	+	-
APS58_1658	*HP*	LRR protein, outer protein XopAC	43	52	*Aave_4632*	+	(+)	(+)
APS58_1676	*HP*	Type III effector protein	not in ML1	25	-	+	+	(+)
APS58_1760	*T3E protein*	Type III effector protein	8	16	*Aave_4728*	+	+	+
APS58_1921	*avrPph3*	Cysteine protease avirulence protein YopT/AvrPphB	61	4	*Aave_0085*	+	+	+
APS58_1966	*xopJ*	Type III effector XopJ	not in ML1	9	-	+	+	+
APS58_2045	*avrRpt2*	Cysteine protease avirulence protein AvrRpt2	156	14	*Aave_0201*	-	-	+
APS58_2122	*xopAG*	Type III effector HopG1/AvrGf1/XopAG	6	10	*Aave_0277*	+	+	+
APS58_2156	*HP*	Type III effector XopC2	951	100	*Aave_0310*	+	+	-
APS58_2228	*HP*	Type III effector SspH1	not in	45	-	(+)	(+)	-

		family	ML1					
APS58_2229	*putative T3E, E3 ligase domain*	Type III effector SspH1 family	not in ML1	50	-	(+)	(+)	-
APS58_2287	*HP*	Type III effector XopK	235	11	*Aave_0433*	+	-	+
APS58_2313	*LRR ribonuclease inhibitor*	LRR type III effector protein (GALA5)	24	71	*Aave_0458*	-	+	-
APS58_2345	*HP*	Type III effector XopP	1161	17	*Aave_0588*	+	+	-
APS58_2589	*HP*	Type III effector YopP/ AvrRxv family	32	5	*Aave_0889*	+	+	(+)
APS58_2767	*HP*	Type III effector protein	not in ML1	64	-	+	+	-
APS58_2799	*HP*	Putative AWR type III effector protein	33	34	*Aave_1090*	-	+	-
APS58_3109	*HP*	Avirulence protein AvrXv3	40	36	*Aave_1373*	+	+	+
APS58_3252	*HP*	Outer protein XopAC	56	118	*Aave_1508*	+	+	-
APS58_3261	*HP*	Type III effector HopBF1	37	60	*Aave_1520*	-	(+)	+
APS58_3289	*hopW1-1*	Type III effector HopW1-1/HopPmaA	15	19	*Aave_1548*	+	+	+
APS58_3303	*HP*	Type III effector XopE2	not in ML1	1	-	+	+	+
APS58_3344	*HP*	Type III effector XopAI	27	93	*Aave_1647*	+	-	(+)
APS58_3751	*mltB_2*	Lytic murein transglycosylase, type III effector HopAJ2	36	285	*Aave_3237*	+	+	+
APS58_3909	*HP*	Type III effector XopV	193	21	*Aave_3085*	+	+	-
APS58_3930	*HP*	Type III effector AvrRxo1-ORF2	655	31	*Aave_3063*	+	-	-
APS58_3931 6	-	Type III effector AvrRxo1	13	-	*Aave_3062*	+	-	-
APS58_3943	*HP*	Type III effector AvrPphF/HopF2	not in ML1	37	-	-	+	+
APS58_4070	*HP*	Type III effector HopH1	7	6	*Aave_2876*	+	+	+
APS58_4101	*HP*	Type III effector, lipase domain	22	22	*Aave_2844*	+	+	-
APS58_4112	*avrBs1*	Avirulence protein AvrBs1/AvrA1	4	7	*Aave_2173*	+	-	+
APS58_4113	*HP*	Avirulence protein AvrBs1/AvrA1	16	2	*Aave_2174*	+	-	+
APS58_4317	*HP*	Type III effector HopD1	34	33	*Aave_2802*	+	+	-

[1] Locus_tag and annotation according to GenBank accession CP029373 [9]. Bolded genes were found to be significantly regulated by HrpX based on RNA-Seq results (S2 Table). *HP*, hypothetical protein.

[2] Similarity based on BlastP analysis of the gene product.

[3] Ranking of the genes in machine learning (ML) runs 1 and 2. ML1 was done with ORFs of *A. citrulli* AAC00-1 (GenBank accession CP000512.1) and ML2 was done with the ORFs *of A.*

citrulli M6 (GenBank accession CP029373). In column ML1, "not in ML1" means that this M6 gene was not detected in ML1 because it has no homologous gene in strain AAC00-1.

[4] Corresponding locus_tag in *A. citrulli* AAC00-1. Underlined genes are the T3E genes that were known prior to this study, based on the annotation of the *A. citrulli* group II strain AAC00-1 [27], in addition of gene *Aave_2708*, which is not present in strain M6.

[5] Similarity to gene products of *Xanthomonas* spp. (X), *Ralstonia* spp. (R) and *Pseudomonas syringae* group (P). + indicates significant similarity to at least one gene product; (+) indicates significant similarity to hits with relatively low query coverage (below 60%); – indicates that no significant hits were detected.

[6] These genes are probably non-functional in strain M6 and in all group I strains assessed so far [27].

An additional insight of this analysis was that most predicted T3E genes of *A. citrulli* share levels of similarity with T3E genes of *Xanthomonas* spp. and *R. solanacearum* (41 and 40 genes, respectively; Table 1). A smaller number of genes, 31, shared similarity with T3E genes of *P. syringae* strains. We also assessed the occurrence of these T3Es in other plant pathogenic *Acidovorax* species (S2 Table). Except for the HopBD1 homolog APS58_1433 that could be detected only in *A. citrulli* strains, the other predicted T3Es occur in other pathogenic *Acidovorax* species, with some of them being widely distributed. For instance, the putative effectors APS58_0492, APS58_0506, APS58_1482, APS58_1657, APS58_1658, APS58_2228, APS58_2313, APS58_2345, APS58_2799, APS58_3303 and APS58_3751 could be detected, at different levels of similarity, in all species. The other putative effectors were restricted to fewer species, with most of them being detected in *A. avenae* strains. While this may reflect the close relatedness between *A. citrulli* and *A. avenae* [30], it is important to consider that, at the time of this analysis, the public database contained 7 and 18 genomes of *A. citrulli* and *A. avenae* strains, respectively, but only two draft genomes of *A. oryzae* and one draft genome for each of the other species.

Interestingly, of the 51 putative T3E genes of *A. citrulli* M6, ten were not present in the genome of the group II strain AAC00-1 (Table 1). Besides M6 and AAC00-1, the NCBI database includes draft genomes of one additional group II strain, KAAC17055, and four group I strains (pslb65, tw6, DSM 17060 and ZJU1106). BlastN analyses revealed that these ten genes are also absent in strain KAAC17055, but present in most of the group I strains. The only exceptions were *APS58_0506* that was not detected in strains tw6 and DSM 17060, *APS58_1209* that was not detected in tw6, and *APS58_2767* that was not detected in DSM 17060. The inability to detect these T3E genes in the genomes of strains tw6 and DSM 17060 could reflect true absence in these strains but also could be due to the draft nature of these genomes. In any case, these results strongly suggest that the ten M6 T3E genes that are absent in the group II strains AAC00-1 and KAAC17055 could be specific to group I strains of *A. citrulli*. Yet, this assumption should be verified on a larger collection of strains. Interestingly, among these ten T3E genes, *APS58_0506*, *APS58_2228* and *APS58_3303*, were detected in strains of all other plant pathogenic *Acidovorax* species (S2 Table). In the case of *APS58_2228*, it should be mentioned that the group II strains AAC00-1 and KAAC17055 possess genes (*Aave_0378* in AAC00-1) that encode short products (140 a.a.) and partially align with the C-terminal region of the group I product (with predicted length of 538 a.a.). In our analysis we did not consider them as ortholog genes.

HrpX is required for pathogenicity of *A. citrulli* M6 and regulates the expression of T3SS components and T3E genes

In *Xanthomonas* spp. and *R. solanacearum*, the transcriptional regulator HrpX (HrpB in *R. solanacearum*) plays a key role in regulation of *hrp* and T3E genes. We

hypothesized that this is also the case in *A. citrulli* M6. To assess this hypothesis, we first generated an *A. citrulli* M6 strain mutated in *APS58_2298*, the *hrpX* orthologous gene. This mutant lost the ability to cause disease in melon (Fig 1A) and induce HR in pepper leaves (Fig 1B), as previously observed for a strain carrying a mutation in the *hrcV* gene, which encodes a core component of the T3SS [10]. A similar loss of pathogenicity was observed for a mutant defected in the *hrpG* homolog gene, *APS58_2299* (S1 Fig). Complementation of both *hrpX* and *hrpG* mutations restored pathogenicity, although necrotic symptoms induced by the complemented strains were less severe than those induced by the wild-type strain (S1 Fig).

Fig 1. HrpX is required for pathogenicity and regulates expression of T3S and T3E genes in *Acidovorax citrulli* M6. (A) Disease lesions produced in a melon leaf inoculated with wild-type M6, but not with mutant strains defective in *hrpX* or *hrcV* (encoding a core component of the T3SS) genes. The picture was taken at 3 days after infiltration (d.a.i.). (B) Cell death observed in a pepper leaf following inoculation with wild-type M6, but not with *hrpX* and *hrcV* mutants. The picture was taken at 4 d.a.i. In (A) and (B), leaves were syringe-infiltrated with bacterial suspension of 10^8 CFU/ml. (C) Qualitative assessment of differential gene expression between wild-type M6 and the M6 *hrpX* mutant after 72 h of growth in XVM2 minimal medium at 28 °C. gDNA, amplification of genomic DNA. cDNA, reverse-trancriptase (RT)-PCR of RNA extracts. Genes: *hrcV* (*APS58_2306*), *hrcT* (*APS58_2309*), *hrcJ* (*APS58_2321*) and *hrcC* (*APS58_2331*), encoding core components of the T3SS; *APS58_3289*, encoding a T3E similar to *Pseudomonas syringae hopW1-1*; and *GADPH*, glyceraldehyde-3-phosphate dehydrogenase (*APS58_1610*; control gene).

Further, we used reverse transcription-PCR (RT-PCR) to compare expression of four genes encoding T3SS components and one T3E gene (*APS58_3289*, encoding a *P. syringae hopW1-1* homolog of *hopW1-1*) between the *hrpX* mutant and wild-type M6 following growth in XVM2 medium. This medium was optimized for expression of T3S

genes in *X. euvesicatoria*, as it simulates, to some extent, the plant apoplast environment [31]. After 72 h of growth, expression of the tested genes was reduced in the *hrpX* mutant relative to wild-type M6 (Fig 1C).

Identification of HrpX-regulated genes by RNA-Seq

Based on RT-PCR results, we carried out RNA-Seq analysis to compare gene expression between wild-type M6 and the *hrpX* mutant, after 72 h of growth in XVM2 medium. This approach revealed 187 genes showing significant differential expression (significant fold-change of ± 2) between the strains (Fig 2A). Of these, 159 genes had significantly reduced expression in the *hrpX* mutant relative to wild-type M6, while 28 genes showed the opposite pattern (S3A and S3B Tables). RNA-Seq results were validated by qPCR experiments that confirmed lower expression of 10 tested genes in the *hrpX* mutant under the same conditions (Fig 2B).

Fig. 2. Comparative transcriptomics analysis between *Acidovorax citrulli* M6 and the M6 *hrpX* mutant. (A) Relative gene expression profile as assessed by RNA-Seq of cells grown for 72 h at 28 °C in minimal XVM2 medium (2 and 3 replicates for the *hrpX* mutant and wild-type strain, respectively). The *A. citrulli* M6 genome map is represented in the external circle. Internal red line shows differential gene expression between the strains. Genes within the gray zone: no significant differences between the strains. The -8 to 2 scale indicates relative expression of the mutant compared with the wild-type. Genes with significantly reduced or increased expression in the mutant relative to the wild-type strain are in the inner and outer regions relative to the gray zone, respectively. Arrows indicate the Hrp-T3SS cluster as well as genes with homology to known effectors from other plant pathogenic bacteria. (B) Relative expression of selected genes by qRT-PCR following bacterial growth under identical conditions as for the RNA-Seq experiment (3 biological replicates per strain). Asterisks indicate significant differences between wild-type and *hrpX* mutant at $\alpha = 5\%$ by the Mann-Whitney non-parametrical test. All tested genes except *APS58_2764* showed

significantly reduced expression in the mutant relative to strain M6 in the RNA-Seq analysis.

Most HrpX-regulated genes could not be assigned to Gene Ontology (GO) categories using Blast2GO. Of the 159 genes that showed reduced expression in the *hrpX* mutant, only 47 were assigned to at least one biological process category. Blast2GO results are detailed in S3C and S3D Tables, and Fig 3 shows the number of biological process categories of genes with reduced expression in the mutant. Among the most frequent categories, 10 hits were found for transmembrane transport proteins, including several ABC transporters and permeases, and 6 matched with regulation of transcription. Nine hits belonged to protein secretion/protein secretion by the T3SS and these corresponded to genes encoding Hrp/Hrc components. Notably, most T3S and T3E genes could not be assigned to any specific GO biological process; this was the case for 11 *hrp*/*hrc*/*hpa* genes and for 24 T3E genes (S3C Table). Overall, RNA-Seq revealed 20 *hrp*/*hrc*/*hpa* genes and 27 genes encoding putative T3Es (including the seven new effectors identified in this study; see below) that had significantly reduced expression in the *hrpX* mutant relative to wild-type M6 (S3B and S3C Tables). Importantly, almost 60 genes that showed reduced expression in the *hrpX* mutant are annotated as hypothetical proteins and did not show similarity to known T3E genes. It is possible that some of these genes encode novel T3Es.

Fig. 3. Distribution of *Acidovorax citrulli* M6 HrpX-regulated genes among categories of biological processes. Of the 159 genes that showed reduced expression in the *hrpX* mutant relative to wild-type M6, only 47 could be assigned to at least one Gene ontology (GO) biological process category (blue columns). HrpX-regulated genes encoding T3S structural and accessory proteins (red column) and putative T3Es (green column) were manually assigned to these categories.

337

338 Interestingly, the *hrpX* mutant also showed reduced expression of several genes
339 encoding proteins that are putatively secreted by the type II secretion system (T2SS).
340 We used SignalP, Pred-Tat and Phobius tools to detect putative Tat or Sec type II
341 secretion (T2S) signals in the ORFs of all genes that showed significantly lower
342 expression in the *hrpX* mutant relative to the wild-type strain. While T2S signals were
343 predicted in 39 genes by at least one of the tools (not shown), 14 genes were predicted
344 to encode products with T2S signals by the three different tools (S3E Table). Among
345 these genes were *APS58_0633* (*xynB*) encoding 1-4-β-xylanase, *APS58_2599* (*pelA_2*),
346 encoding pectate lyase, and *APS58_3722*, encoding a family S1 extracellular serine
347 protease. These three genes were also shown to contain PIP boxes in their promoter
348 region (S3B Table).

349 Of the 28 genes showing increased expression in the *hrpX* mutant relative to
350 wild-type M6, only ten could be assigned to GO categories, most of which belonged to
351 regulatory genes (regulation of transcription, phosphorelay signal transduction system,
352 signal transduction; S3D Table).

353

354 **Identification of PIP boxes in HrpX-regulated genes**

355 We used fuzznuc to search for perfect PIP boxes in the *A. citrulli* M6 genome,
356 using the consensus sequence TTCGB-N15-TTCGB. Based on Koebnik *et al.* [32], we
357 considered only those cases for which the distance between the end of the PIP box and
358 the putative start codon was shorter than 650 nucleotides. This screen revealed a total of
359 78 PIP boxes (S4 Table), of which 41 correlated with significant regulation by HrpX
360 (Table 2 and S4 Table). We used the PIP boxes of the aforementioned 41 genes/operons
361 to determine the consensus PIP box of *A. citrulli* using the MEME suite (Fig 4).

Importantly, some of the PIP boxes are upstream of operons, thus probably regulating the expression of more than one gene. We detected additional 25 genes [marked as (+) in the PIP box column of S3B Table] that are likely in PIP box-containing operons and showing higher expression in the wild-type strain relative to the *hrpX* mutant. It is also worth mentioning that eleven additional genes (some of which encoding T3Es) carrying PIP boxes showed higher expression values in the wild-type relative to the *hrpX* mutant in the RNA-Seq experiment, but were slightly below the level of statistical significance (S3A and S4 Tables).

Table 2. Perfect plant-inducible promoter (PIP) box sequences in genes that were shown to be regulated by HrpX in *Acidovorax citrulli* M6.

Gene_ID[1]	Annotation[1]	Strand	PIP box[2]	Start of PIP box	End of PIP box	Gene start codon	Distance (bp)[3]
APS58_0030	*HP*	-	ttcgttttgttgattggaaattcgc	34554	34578	34553	1
APS58_0077	*HP*	-	ttcgcaattcgagaaatttgttcgg	93187	93211	93022	165
APS58_0185	*HP*	-	ttcgtgttgaaggcattcgtttcgg	216423	216447	216315	108
APS58_0197	*puuD_1*	-	ttcgtgcatcggctcttccattcgc	227069	227093	226515	554
APS58_0218	*HP*	-	ttcgcgtgtgcgtgaactctttcgc	254146	254170	254075	71
APS58_0500	*HP*	-	ttcgccccggcctgccggacttcgc	579574	579598	579502	72
APS58_0502	*yopJ*	-	ttcgcccggcaggcacccgtttcgc	583025	583049	582809	216
APS58_0543	*HP*	-	ttcgcatgcatgtgagcggattcgg	631454	631478	630839	615
APS58_0633	*xynB*	-	ttcgcttgctgcttcacgggttcgc	715951	715975	715863	88
APS58_0886	*HP*	-	ttcgcatcgccgtgcatggtttcgc	1015878	1015902	1015701	177
APS58_0986	*HP*	+	ttcgcattccgcgcgactgcttcgc	1113649	1113673	1113709	36
APS58_1000[4]	*HP*	+	ttcgccaccgggcgcacggcttcgt	1129783	1129807	1129817	10
APS58_1026	*HP*	-	ttcgtgcacgcgcctgccggttcgc	1161953	1161977	1161806	147
APS58_1255	*HP*	+	ttcgcgcgccacggccccgcttcgc	1409795	1409819	1410119	300
APS58_1340	*HP*	+	ttcgcatgtccgcggagtcgttcgg	1511860	1511884	1512052	168
APS58_1448	*HP*	-	ttcgcgaggccacgcattgcttcgc	1632395	1632419	1632309	86
APS58_1483	*HP*	-	ttcgcattcccgtggccggcttcgg	1669735	1669759	1669644	91
APS58_1760	*T3E protein*	+	ttcgtgcctgcgggcacgtattcgc	1970321	1970345	1970408	63
APS58_1954	*HP*	+	ttcgcaagttctccagcttttcgg	2174442	2174466	2174654	188
APS58_1986	*HP*	-	ttcgcgccagcgcgcgggacttcgc	2212320	2212344	2212063	257
APS58_2304	*hrcQ*	-	ttcgccttacgcgatgagccttcgg	2546196	2546220	2546073	123
APS58_2307	*hrcU*	-	ttcgcgcggggcggaaccgcttcgc	2550224	2550248	2550146	78
APS58_2308	*hrpB7*	+	ttcgcattccggtgcgcggcttcgg	2550284	2550308	2550387	79
APS58_2312	*hrpW*	+	ttcgcatccgctgcgccgccttcgc	2553056	2553080	2553423	343
APS58_2314	*HP*	+	ttcgcgatgccgcatgcagcttcgc	2556756	2556780	2556924	144
APS58_2329	*HP*	-	ttcgcaagccatgaagcaacttcgt	2567741	2567765	2566734	7
APS58_2331	*hrcC*	-	ttcgcaagccgtcgcgcggcttcgc	2569879	2569903	2569803	76
APS58_2345	*HP*	+	ttcgcgcaaaggtgagcggcttcgc	2581209	2581233	2581585	352
APS58_2347	*HP*	+	ttcgcaccgccgtgcaggggttcgc	2585239	2585263	2585399	136
APS58_2599	*pelA_2*	-	ttcggctgcatggccgccgcttcgc	2862541	2862565	2862501	40
APS58_2771	*HP*	+	ttcggaccgctgcgccggcattcgc	3052001	3052025	3052432	407
APS58_2974	*HP*	-	ttcgttccaggcaggctgtcttcgc	3262651	3262675	3262590	61
APS58_3261	*HP*	+	ttcgcctggcgcaatgcgggttcgc	3574633	3574657	3574825	168
APS58_3289	*hopW1-1*	-	ttcgccggggagggcagtttttcgc	3605458	3605482	3605197	261

APS58_3297	*HP*	-	ttcgcggggtggcactccgcttcgg	3611673	3611697	3611575	98
APS58_3344	*HP*	-	ttcgcagccctccccggcacttcgc	3656278	3656302	3656147	131
APS58_3685	*HP*	-	ttcgcacgttggacatgcatttcgc	3989762	3989786	3989700	62
APS58_3722	*HP*	+	ttcgttttaagacgaagaaattcgc	4030992	4031016	4031209	193
APS58_4095	*HP*	+	ttcgcatccatggggccggcttcgc	4442672	4442696	4443213	517
APS58_4116	*HP*	-	ttcgcgcaggcgcatgcgcgttcgc	4476037	4476061	4475953	84
APS58_4317	*HP*	-	ttcgcaccgtcggccatcgcttcgc	4692889	4692913	4692529	360

[1] Locus_tag and annotation according to GenBank accession CP029373. *HP*, hypothetical protein.

[2] PIP box consensus: TTCGB-N15-TTCGB (where B is any nucleotide except adenine).

[3] Distance between the end of the PIP box and the first nucleotide of the start codon.

[4] Gene *APS58_1000**: this gene was not annotated in the new M6 annotation. It is located between genes *APS58_0999* and *APS58_1000* (positions 1129817-1130383), and its expression was confirmed by RNA-Seq.

Fig. 4. Sequence logo of the *Acidovorax citrulli* M6 plant-inducible promoter (PIP) box motif. The logo was generated with MEME-ChiP based on multiple alignment of the 41 perfect PIP boxes that were found to be associated with HrpX-regulated genes by RNA-Seq (see Table 2).

Establishment of a translocation assay for validation of *A. citrulli* T3Es

A critical prerequisite for the discovery of new T3Es is the availability of a suitable translocation assay. We assessed the possibility of exploiting the *avrBs2-Bs2* gene-for-gene interaction to test translocation of predicted *Acidovorax* T3Es into plant cells. The *X. euvesicatoria* AvrBs2 effector elicits an HR in pepper plants carrying the *Bs2* resistance gene [33]. A truncated form of this effector, carrying amino acids 62-574 ($AvrBs2_{62-574}$), lacks the N-terminal T3S translocation signal, but retains the ability to elicit the HR when expressed in *Bs2* pepper cells [34]. The *avrBs2-Bs2* translocation assay is thus based on generation of plasmids carrying the candidate T3E (CT3E) genes fused upstream and in frame to the $AvrBs2_{62-574}$. The plasmid is then mobilized into a *X. euvesicatoria* 85-10 *hrpG*ΔavrBs2* strain, that constitutively expresses *hrpG* and lacks *avrBs2*. The resulting strain is used to inoculate leaves of the pepper line ECW20R that

carries the *Bs2* gene. If the AvrBs2$_{62-574}$ domain is fused with a T3E gene, this elicits a *Bs2*-dependent HR [34]. Teper *et al.* recently used this reporter system to validate novel T3Es of the *X. euvesicatoria* strain 85-10 [28].

Given the close similarity between the T3SSs of *A. citrulli* and *Xanthomonas* spp., we hypothesized that the *X. euvesicatoria* T3S apparatus would recognize and translocate *A. citrulli* T3Es, and therefore, that the *avrBs2-Bs2* reporter system would be suitable for validating *A. citrulli* CT3E genes. To assess this hypothesis, we tested translocation of eight T3Es of *A. citrulli* showing similarity to known T3Es of other plant pathogenic bacteria. All tested fusions were translocated into pepper cells in a T3S-dependent manner and induced a *Bs*2-dependent HR in ECW20R pepper leaves. In contrast, HR was not detected when the fusions were tested in ECW30 leaves (lacking the *Bs2* gene), and when a *X. euvesicatoria hrpF* mutant (impaired in T3S) was used in these assays (Fig 5A). Overall, these results demonstrated the suitability of the *avrBs2-Bs2* assay for validation of *A. citrulli* CT3Es.

Fig. 5. Translocation assays of T3Es of *Acidovorax citrulli* M6. (A) Selected T3Es based on sequence similarity to T3Es from other plant pathogenic bacterial species (see Table 1). (B) Candidate T3Es (CT3Es) selected from ML and RNA-Seq analyses. T3E/CT3E ORFs were cloned in plasmid pBBR1MCS-2 upstream to the AvrBs2$_{62-574}$ domain, which elicits HR in ECW20R pepper plants carrying the *Bs2* gene, but not in ECW30R pepper plants that lack this gene. The plasmids were transformed into *Xanthomonas euvesicatoria* 85-10-*hrpG*-ΔavrBs2*, and the resulting strains were used to inoculate pepper plants. All known T3Es (A) and seven among eleven tested CT3Es (B) elicited HR in ECW20R but ECW30R leaves, similarly to the positive control XopS-AvrBs2$_{62-574}$. Infiltrated areas are surrounded by red circles. No HR was induced when leaves were inoculated with a *X. euvesicatoria* mutant impaired in T3S (*ΔhrpF*) expressing T3E/CT3E-AvrBs2$_{62-574}$ fusions. Also, no HR was induced following inoculation with *X. euvesicatoria* 85-10-*hrpG*-ΔavrBs2* without any plasmid (not shown) or with a plasmid expressing the AvrBs2$_{62-574}$ domain alone (ΔN-terminal).

Numbers at the top correspond to the locus_tag in strain M6 (for example, 0492 is gene *APS58_0492*).

Seven novel T3Es of *A. citrulli* are translocated into plant cells

Following validation of the *avrBs2-Bs2* reporter assay for *A. citrulli* T3Es, we selected seven CT3Es based on results from the first ML run and RNA-Seq analysis. Four genes that were ranked relatively low in the ML were also included in these experiments to evaluate the quality of the ML prediction (Table 3 and S1 Table). All seven CT3E genes, but not the low-ranked ML genes, were translocated (Fig 5B). The validated genes were annotated as hypothetical proteins, had a predicted PIP box, were shown to be positively regulated by HrpX, and ranked high in the ML run (Table 3 and S1 Table). Importantly, the gene *APS58_1340*, which contains a PIP box in its promoter region and its expression is regulated by HrpX (Table 3) was not translocated, indicating that these two parameters alone are not sufficient for accurate prediction of T3Es.

Table 3. Candidate T3E genes of *Acidovorax citrulli* M6 that were tested in the *avrBs2-Bs2* translocation assays.

Gene ID[1]	Product	ML[2]	PIP[3]	RSEQ[4]	TRA[5]
APS58_0500	Hypothetical protein[7]	39/48	+	+	+
APS58_0705	GrxD, glutaredoxin-4	91/2203	-	-	-
APS58_0863	Hypothetical protein	64/749	-	-	-
APS58_1000*[6]	Hypothetical protein[7]	21/*	+	+	+
APS58_1340	Hypothetical protein	84/535	+	+	-
APS58_1448	Hypothetical protein[7]	17/104	+	+	+
APS58_2974	Hypothetical protein[7]	19/29	+	+	+
APS58_3297	Hypothetical protein[7]	20/61	+	+	+
APS58_4095	Hypothetical protein[7]	31/46	+	+	+
APS58_4116	Hypothetical protein[7]	11/43	+	+	+
APS58_4399	Hypothetical protein	174/739	-	-	-

[1] Gene IDs are according to the annotation of the *A. citrulli* M6 chromosome (GenBank accession CP029373).

[2] ML: rankings in first/second machine learning (ML) runs. *, gene *APS58_1000** was not included in the second ML run (see below).

[3] PIP: presence (+) or absence (-) of perfect plant-inducible promoter (PIP) box in the promoter region.

[4] RSEQ: significantly reduced expression in the *hrpX* mutant relative to the wild type (+)/no significant differences between strains (-).

[5] TRA: translocated (+)/non-translocated (-) in *avrBs2-Bs2* translocation assays (rows of validated genes are shaded with gray).

[6] *APS58_1000**: this gene ranked high in the first ML but was not annotated in the recent annotation of *A. citrulli* M6, although its expression was confirmed by RNA-Seq. Its ORF is located between genes *APS58_0999* and *APS58_1000* (positions 1129817-1130383).

[7] These genes were detected only in plant pathogenic *Acidovorax* species.

BlastP analyses of the seven newly identified T3E genes revealed strong similarity only to hypothetical proteins of plant pathogenic *Acidovorax* species. The fact that no homologs for these genes were detected in non-pathogenic *Acidovorax* strains (despite the availability of more than 70 genomes of such spp.) or in other plant pathogenic bacterial species suggests a specific and unique role for their products in *Acidovorax* pathogenicity. These seven genes were detected also in AAC00-1 (S2 Table) and in all other group I and II genomes available in NCBI. Some of them were widely distributed among other plant pathogenic *Acidovorax* species. For instance, *APS58_4095* was also detected in *A. oryzae* and in *A. cattleyae*, and homologs with less than 60% query coverage were also present in *A. konjaci*, *A. anthurii* and *A. valerianellae*. In contrast, *APS58_2974* was not detected in *Acidovorax* spp., other than *A. citrulli* and *A. avenae* (S2 Table). Searches for conserved domains in these T3Es did not provide any insight.

Assessment of localization of three of the newly identified T3Es

We attempted to assess the subcellular localization of three of the newly identified T3Es, APS58_0500, APS58_1448 and APS58_4116. Prediction of subcellular localization using the Plant-mPLoc server indicated that the three effectors could localize to the nucleus. Browsing these T3Es with the LogSigDB server revealed endoplasmic reticulum (ER) localization signals in the three effectors, and nuclear localization signals in APS58_0500 and APS58_4116.

We assessed localization of these effectors fused to the yellow fluorescent protein (YFP) in *Nicotiana benthamiana* leaves following transient expression by agroinfiltration. Based on the aforementioned predictions, in first experiments the leaves were co-infiltrated with *A. tumefaciens* carrying the ER marker mRFP-HDEL, and were also stained with DAPI for nucleus localization. Representative images from these experiments are shown in Fig 6. The results suggested that the three effectors could interact with the ER, but only APS58_0500 and APS58_1448 partially localized to the nucleus, including in clearly visible nuclear foci (Fig 6).

Fig. 6. Transient expression of *Acidovorax citrulli* T3Es in *Nicotiana benthamiana*. The T3E genes *APS58_0500*, *APS58_4116* and *APS58_1448*, identified by ML and RNA-Seq and validated in translocation assays, were cloned in the binary vector pEarleyGate101, fused to the C-terminus of YFP. The plasmids were transformed into *Agrobacterium tumefaciens* GV3101, and the resulting strains were used for transient expression in *N. benthamiana*. Leaves were co-inoculated with *A. tumefaciens* GV3101 carrying the mRFP-HDEL endoplasmic reticulum marker and stained with DAPI for visualization of plant cell nuclei. Samples were visualized in a Leica SPE confocal microscope 48 h after inoculation. Bars at the right bottom of each picture, 20 µm.

In a second set of experiments, the YFP-fused effectors were co-infiltrated with free-mCherry, localized mainly in the cytosol and in the nucleus, HDEL-mCherry, localized to the ER, and the membrane-bound protein SlDRP2A (L. Pizarro and M. Bar,

503 unpublished results). Representative images from these experiments are shown in S2-
504 S4 Figs for APS58_0500, APS58_1448 and APS58_4116, respectively. The three
505 effectors partially co-localized with the membrane-bound protein SIDRPA, as
506 evidenced by the Pearson correlation coefficients (0.40±0.024 for APS5_0500,
507 0.49±0.040 for APS58_1448, and 0.53±0.037 for APS58_4116). Since APS58_0500
508 appeared to have a stronger membrane localization, we used the classical plasma
509 membrane microdomain protein Flot1 [35] as an additional membrane control marker.
510 Indeed, APS58_0500 had an expression pattern that was highly similar to that of Flot1
511 (compare top and bottom panels in S2 Fig). In agreement with the first set of
512 experiments (Fig 6), APS58_0500 (S2 Fig) and APS58_1448 (S3 Fig) partially
513 localized to the nucleus. On the other hand, these experiments confirmed that only
514 APS58_4116 partially interacted with the ER, mostly at the nuclear envelope (Fig 6 and
515 S4 Fig; Pearson coefficient with HDEL-mCherry 0.53±0.037). None of the effectors
516 was shown to have a significant cytosolic presence: the Pearson coefficient with
517 mCherry was lower than 0.12 for APS_0500 and APS_4116, while for APS_1448 the
518 coefficient was 0.53±0.037, due to the strong nuclear presence of this effector, as
519 indicated above. Overall, we can conclude that the three effectors are associated with
520 the plasma membrane, APS58_0500 and APS58_1448 partially localize to the nucleus,
521 and APS_4116 partially interacts with the ER.
522
523 **Generating an improved list of candidate T3Es of *A. citrulli* M6 with a second ML**
524 **run**
525 Machine learning can be improved after refinement of features specific to the
526 studied pathogen. Thus, we carried out a second ML run using the *A. citrulli* M6
527 genome. The main differences between the first and second ML runs were: (i) the

second run was done on the M6 genome [9], which by this time was fully assembled; (ii) we included the seven novel T3Es identified in this study in the positive set and the four ORFs that were found not to be translocated were added to the negative set; (iii) in the positive set we included ORFs with high sequence similarity to known effectors from other bacteria, based on our homology search results (Table 1); and (iv) we used HrpX-mediated regulation as an additional feature used to train the classifier. The results are summarized in S5 Table. Most known/validated T3Es ranked among the top 100 hits, and among the top 40 hits, 34 were known/validated T3Es. Importantly, some genes with high propensity to encode T3Es (ranking among the top 60 in the second ML run) did not appear among the top 200 hits in the first ML list (Table 1 and S1 Table), thus supporting the higher reliability of the new list relative to the first prediction.

Among the top 100 hits of the second ML run, there were 37 genes that matched to hypothetical proteins from the public database, with no similarity evidence to suggest a T3E nature. Since this was the case of the seven T3Es validated in this study, it is possible that some of these genes encode previously undiscovered T3Es. In this regard, it is worth mentioning genes *APS58_1954*, *APS58_1986*, *APS58_3685*, *APS58_0987* and *APS58_1694* (ranking at positions 20, 27, 57, 62 and 83 in the second ML, respectively). While *APS58_1694* shares similarity only with hypothetical proteins of plant pathogenic *Acidovorax* species, the first four also share similarities to hypothetical proteins of other plant pathogenic genera (eg., *Xanthomonas*, *Ralstonia*, *Pseudomonas* and/or *Erwinia*). These genes also showed increased expression in wild-type M6 relative to the *hrpX* mutant, and have PIP boxes in their promoter region. Therefore, these genes are strong candidates for further experimental validations.

Discussion

553 Type III effectors (T3Es) play a dual role in the interaction between many Gram-
554 negative plant pathogenic bacteria and plants: while they collectively promote virulence
555 on susceptible plants, some may induce effector-triggered immunity (ETI) in plants
556 carrying the corresponding resistance (*R*) genes. *R* genes provide resistance against
557 economically important pathogens and have been mobilized to commercial crop
558 varieties by breeding programs. Thus, this is one of the most important means of disease
559 management [36, 37].

560 *Acidovorax citrulli* requires a functional type III secretion (T3S) system for
561 pathogenicity [10]. The main objective of this study was to significantly advance the
562 current knowledge about the arsenal of T3Es of *A. citrulli*. Among well-investigated
563 plant pathogenic bacteria, the pools of T3Es vary from only few effectors in
564 phytopathogenic bacteria from the *Enterobacteriaceae* family, to approximately 20 to
565 40 in strains of *P. syringae* and *Xanthomonas* spp. [21, 28, 40-44] and an average of
566 over 75 in *R. solanacearum* isolates [45, 46]. Thus, we hypothesized that the repertoire
567 of *A. citrulli* T3Es could be much larger than the eleven T3E genes identified in the
568 group II strain AAC00-1 [27].

569 As a first approach to uncover the arsenal of *A. citrulli* T3Es, we used a genome-
570 wide machine learning (ML) algorithm to determine the propensity of ORFs to encode
571 T3Es. In parallel, we looked carefully at the annotation of the group I model strain of *A.*
572 *citrulli*, M6, and carried out BlastP analyses of the genes encoding hypothetical proteins
573 or functions that could infer effector activity. These analyses revealed 51 putative T3E
574 genes that shared different levels of similarity with known effector genes from
575 *Xanthomonas* spp., *R. solanacearum* and/or *P. syringae* strains (Table 1). Homologs for
576 most of these T3E genes and for those identified in the present study were also detected
577 in other plant pathogenic *Acidovorax* species (S2 Table).

To identify new T3E genes of *A. citrulli*, we also used RNA-Seq to identify HrpX-regulated genes. Based on the knowledge accumulated with *Xanthomonas* spp. and *R. solanacearum* [22, 32, 47, 48], we expected that most genes encoding T3SS components and some T3Es of *A. citrulli* would be under the direct regulation of HrpX. This assumption was strengthened in preliminary experiments comparing gene expression between a wild-type and a *hrpX* mutant strain (Fig 1C). As previously mentioned, Zhang *et al.* recently showed that HrpX controls the expression of one T3E gene in the group II strain, Aac5 [26].

The RNA-Seq approach revealed 159 genes showing significantly reduced expression in the *hrpX* mutant, while 28 genes had significantly increased expression in the mutant (S3 Table). These numbers are similar to those reported in gene expression studies carried out with *Xanthomonas* spp. HrpX and with *R. solanacearum* HrpB. For instance, microarray analyses of *Xanthomonas axonopodis* pv. *citri* (*Xac*) in XVM2 medium revealed that 181 genes were up-regulated by HrpX, while 5 to 55 genes (depending on the time point) were down-regulated by this transcriptional regulator [47]. Occhialini *et al.* found 143 HrpB up-regulated genes and 50 HrpB down-regulated genes in *R. solanacearum* [48]. In these, as well as in several other studies, HrpX/HrpB was found to regulate the expression of most genes encoding T3S components and accessory proteins as well as several T3E genes [21, 22, 49]. In line with this background, among the 159 HrpX up-regulated genes found in our study, 20 encoded *hrp*/*hrc*/*hpa* genes and 27 encoded T3E genes. Interestingly, *hrcC* was a member of the *A. citrulli* HrpX regulon. *hrcC* expression in *X. euvesicatoria* is directly regulated by HrpG, in an HrpX-independent manner [31]. In contrast, in *R. solanacearum*, *hrcC* is regulated by HrpX [49, 50] as we found in *A. citrulli* M6.

In *Xanthomonas* spp. and in *R. solanacearum*, the HrpX/HrpB regulon includes many genes that are not involved in T3S [21, 47, 49]. A similar picture emerged from our study, where HrpX was shown to regulate genes involved in transmembrane transport, including several ABC transporters and permeases as well as transcriptional regulators. Among the HrpX up-regulated genes we also detected several genes whose products are putatively secreted by type II secretion (T2S). These included genes encoding 1-4-β-xylanase (*xynB*), pectate lyase and a protein with similarity to a family of S1 extracellular serine proteases (S3E Table). HrpX regulation of genes encoding type II-secreted enzymes was also demonstrated in *Xanthomonas* spp. and in *R. solanacearum* [22, 47, 51-54].

Among the 159 HrpX up-regulated genes *in A. citrulli*, more than 60 carried perfect PIP boxes in their promoter region or were part of operons carrying perfect PIP boxes (Table 2; S3 and S4 Tables). Although some other genes may carry imperfect PIP boxes and may be directly regulated by HrpX, this result suggests that many of the HrpX up-regulated genes are indirectly regulated by this transcriptional factor. This is a reasonable assumption, considering that among the genes that are up- and down-regulated by HrpX, there are several transcriptional regulators. For instance, genes encoding transcriptional factors belonging to the LysR (*APS58_0949* and *APS58_2039*), IclR (*APS58_1263*), FmbD (*APS58_1340*) and TetR (*APS58_3638*) families were shown to be up-regulated by HrpX. In contrast, two genes encoding DNA-binding response regulators, homologous to PhoP (*APS58_0821*) and FixJ (*APS58_1682*) were HrpX-down-regulated (S2B Table).

After demonstrating the suitability of the *avrBs2-Bs2* T3E translocation assay with eight known T3Es, we used the data obtained from the first ML run and the RNA-Seq analysis to select seven *A. citrulli* M6 ORFs for experimental validation (Fig 5). We

validated translocation of the seven candidates, thus demonstrating the strength of combining ML and RNA-Seq for identifying T3E genes. Importantly, the lack of translocation of the four ORFs that received relatively low scores in the first ML run strengthened the suitability of our combined computational/experimental approach.

Remarkably, the seven effectors identified in this study were up-regulated by HrpX and carried PIP boxes in their promoter regions, while among the four non-validated genes, only one had these traits (Table 3). An interesting trait of the seven new T3Es was that they share significant similarity only with hypothetical proteins of other plant pathogenic *Acidovorax* strains (Table 3 and S2 Table). This strongly supports that these effectors are unique to plant pathogenic *Acidovorax*. Importantly, a second ML run, informed by the knowledge accumulated from this study, revealed additional genes that were ranked in relatively high positions and encoded hypothetical proteins that occur only in plant pathogenic *Acidovorax* or in other plant pathogenic bacteria (S5 Table). These represent high priority CT3Es for future experimental validation assays. This emphasizes one benefit of the ML approach: its ability to integrate novel knowledge in the prediction algorithm.

Another interesting characteristic of the new T3Es discovered in this study is their relatively small size. Based on the annotation of the M6 genome, the average and median lengths of *A. citrulli* M6 T3Es are 387.7 and 345 amino acids (a.a.), respectively. Except for *APS_4116* that encodes a 347-a.a. protein, the size of the six other new T3Es ranged from 113 a.a. (APS58_4095) to 233 a.a. (APS58_0500) (S5 Fig). In the public database (GenBank), there are several examples of small T3Es from plant pathogenic bacteria, including *Xanthomonas* AvrXv3 (most having 119 a.a.), *Pseudomonas syringae* HopAF1 (112-291 a.a.), HopBF1 (125-207 a.a.), HopF2 (177-

280 a.a.), HopH1 (201-218 a.a.) and AvrRpt2 (222-255 a.a.), and the *R. solanacearum*/*Xanthomonas* HopH1 homologs (155-218 a.a.).

In this study we assessed plant cell localization of three of the new T3Es validated in translocation assays, APS58_0500, APS58_1448 and APS58_4116. Utilization of subcellular localization prediction tools and confocal microscopy of *N. benthamiana* agro-infiltrated leaves strongly suggest that the three tested effectors interact with the plasma membrane (S2-S4 Figs), with APS58_0500 remarkably mimicking the localization of the classical non-clathrin mediated endocytic system protein, Flot1 [35]. While APS58_4116 interacted with the endoplasmic reticulum (Fig 6 and S2 Fig), effectors APS58_0500 and APS58_1448 partially localized to the nucleus (Fig 6; S3 and S4 Figs). Interestingly, and in line with the predicted nuclear localization of these effectors, BlastP showed that APS58_0500 has low similarity with an ATP-dependent RNA helicase of the Metazoa organism *Clonorchis sinensis* (query cover, 38%; e-value, 0.23), while APS58_1448 has low similarity to a transcriptional regulator of the bacterium *Hoeflea halophila* (query cover, 54%; e-value, 0.19-0.53), suggesting possible functions the *Acidovorax* effectors might execute upon entrance into the plant cell nucleus.

In conclusion, we have combined sequence analysis, ML and RNA-Seq approaches to uncover the arsenal of T3Es of the group I model strain of *A. citrulli*, M6, including discovery of new T3Es that appear to be unique to plant pathogenic *Acidovorax* spp. Further characterization of the novel T3Es identified in this study may uncover new host targets of pathogen effectors and new mechanisms by which pathogenic bacteria manipulate their hosts. We also demonstrated the suitability of a translocation reporter system for validation of *A. citrulli* T3Es, which we expect, will be very helpful to the *Acidovorax* research community. Until recently it was assumed that

676 *A. citrulli* strains (and in general plant pathogenic *Acidovorax* strains) possess little over
677 ten T3E genes. However, from this study it is clear that the *A. citrulli* pan-genome
678 encodes more than 50-60 T3Es. Therefore, the *A. citrulli* T3E repertoire is larger than
679 those of most well-characterized plant pathogenic bacteria, including plant pathogenic
680 *Enterobacteria*, *P. syringae* pathovars, *Xanthomonas* spp. and, and closer in numbers to
681 the T3E repertoires of *R. solanacearum*. Moreover, the second ML run suggested that *A.*
682 *citrulli* may possess yet unrevealed T3E genes. Importantly, among the 58 known T3E
683 genes of *A. citrulli* M6, ten (17.2%) appear to be unique to group I strains. On the other
684 hand, the group II model strain, AAC00-1, carries T3E genes that are absent or non-
685 functional in group I strains as shown in our previous report [27] and in this study
686 (Table 1 and S1 Table). Thus, it is logical to assume that the variability in T3E content
687 between group I and II strains plays a critical role in shaping the differences in host-
688 preferential association between the groups. Despite this, more research is needed to test
689 this hypothesis, and to understand the mode of action and contribution of individual
690 effectors to the virulence of *A. citrulli*.
691

692 # Methods

693 ## Bacterial strains and plasmids

694 Bacterial strains and plasmids used in this study are listed in S6 Table. Unless
695 stated otherwise, *Acidovorax citrulli* strains were grown at 28 ºC in nutrient broth (NB;
696 Difco Laboratories, Detroit, Michigan) or nutrient agar (NA; NB containing 15 g/L
697 agar). For RT-PCR, qRT-PCR and RNA-seq experiments, *A. citrulli* strains were grown
698 in XVM2 medium [31]. *Xanthomonas euvesicatoria*, *Agrobacterium tumefaciens* and
699 *Escherichia coli* strains were cultured on Luria-Bertani (LB) medium [55] at 28 ºC for
700 *X. euvesicatoria* and *A. tumefaciens*, and 37 ºC for *E. coli*. When required, media were

supplemented with the following antibiotics: ampicillin (Ap, 100 µg/mL for *E. coli* and 200 µg/mL for the others), rifampicin (Rif, 50 µg/mL), kanamycin (Km, 50 µg/mL), and gentamycin (Gm, 50 µg/mL for *A. citrulli* and 10 µg/mL for the others).

Molecular manipulations

Routine molecular manipulations and cloning procedures were carried out as described [55]. T4 DNA ligase and restriction enzymes were purchased from Fermentas (Burlington, Canada). AccuPrep® Plasmid Mini Extraction Kit and AccuPrep® PCR Purification Kit were used for plasmid and PCR product extraction and purification, respectively (Bioneer Corporation, Daejeon, Republic of Korea). DNA was extracted with the GeneElute bacterial genomic DNA Kit (Sigma-Aldrich, St. Louis, MO, USA). PCR primers were purchased from Sigma-Aldrich and are listed in S7 Table. PCR reactions were performed with the Readymix Red Taq PCR reactive mix (Sigma-Aldrich) or with the Phusion high-fidelity DNA polymerase (Fermentas, Waltham, MA, USA) using an Eppendorf (Hamburg, Germany) thermal cycler. Sequencing of PCR fragments and constructs was performed at Hy Laboratories (Rehovot, Israel). *Escherichia coli* S17-1 λpir, DH5-α and DB3.1 strains were transformed using an Eppendorf 2510 electroporator according to manufacturer's instructions. Plasmid mobilizations to *A. citrulli* and *X. euvesicatoria* strains were done by bi-parental mating as described [56]. *A. tumefaciens* cells were transformed by the heat shock method [57].

Machine learning classifications

In order to predict T3Es, we applied ML classification algorithms, which are similar to the ones we have previously described [28, 29, 58, 59]. The first ML run was used to search for T3Es in the AAC00-1 genome (GenBank accession CP000512.1).

The training data included 12 ORFs that were known as T3Es (see in Results). The negative set included 2,680 ORFs that had high similarity (E-value less than 0.001) to ORFs in the non-pathogenic *E. coli* K12 genome (accession number NC_000913.3). The positive and negative ORFs are marked in S1 Table. For this ML, 71 features were used, including homology (to known effectors or to bacteria without T3SS), composition (amino acid composition, GC content), location in the genome (e.g., distance from known T3Es), and the presence of a PIP box in the promoter region. The complete list of features is given in S8 Table. Features were extracted using in-house Python scripts. The outcome of the ML run is a score for each ORF, reflecting its likelihood to encode a T3E. We evaluated several classification algorithms: random forest [60], naïve Bayes [61], support vector machine (SVM; [62]), K nearest neighbors (KNN), linear discriminate analysis (LDA), logistic regression (all three described in Hastie *et al*. [63]), and Voting, which aims to predict averaging over all other ML algorithms. For each run, feature selection was performed. The ML algorithms and feature selection were based on the Scikit-learn module in Python [64]. The area under the curve (AUC) score over 10- fold cross- validation was used as a measure of the classifier performance. The first ML run was based on the random forest classifier which gave the highest AUC (0.965).

The second ML run was similar to the first, with the following modifications. First, the classifiers were run on the M6 genome (GenBank accession CP029373). Second, the positive set included ORFs that were validated as T3Es in this study and ORFs with high sequence similarity to known effectors as described in Table 1. The negative set included 2,570 ORFs (S5 Table). The four ORFs that were experimentally shown not to be T3Es were also included in this negative set. Third, the expression data from the RNA-Seq analysis (HrpX regulation) were added as a feature. Fourth, the PIP

box feature was updated to reflect the PIP box as inferred from promoter regions of *Acidovorax* T3Es (see additional bioinformatics tools below). The second ML run was based on Voting classifier, which included all the classifiers specified above, as it gave the highest AUC among all the classifiers. The AUC for this second ML run was 0.999.

Generation of *A. citrulli* mutants and complemented strains

Acidovorax citrulli M6 mutants disrupted in *hrpX* (*APS58_2298*) and *hrpG* (*APS58_2299*) genes were generated by single insertional mutagenesis following single homologous recombination. Internal fragments of the *hrpX* (383 bp) and *hrpG* (438 bp) ORFs carrying nucleotide substitutions that encode early stop codons, were PCR-amplified and inserted into the *Bam*HI/*Eco*RI site of the suicide plasmid pJP5603 [65]. The resulting constructs were transformed into *E. coli* S17-1 λpir, verified by sequencing, and mobilized into *A. citrulli* M6 by bi-parental mating. Transconjugants were selected by Km selection. Disruption of the target genes by single homologous recombination and plasmid insertion was confirmed by PCR and sequencing of amplified fragments. To generate complemented strains for mutants disrupted in *hrpX* and *hrpG* genes, the full ORFs of these genes (1407 pb and 801 bp, respectively) were PCR-amplified and cloned into the *Eco*RI/*Bam*HI sites of pBBR1MCS-5 [66]. The generated plasmids were transformed into *E. coli* S17-1 λpir, verified by sequencing, and transferred by bi-parental mating into the corresponding M6 mutant strains. Complemented strains were selected by Gm resistance and validated by PCR.

Infiltration of melon and pepper leaves with *A. citrulli* strains

Melon (*Cucumis melo*) cv. HA61428 (Hazera Genetics, Berurim, Israel) plants were grown in a greenhouse at ~28 °C. Pepper (*Capsicum annum*) cv. ECW20R and

776 ECW30 [67] plants were grown in a growth chamber (16 h/26 °C in the light; 8 h/18 °C
777 in the dark; relative humidity set to 70%). The three youngest, fully expanded leaves of
778 3-week-old melon and 5-week-old pepper plants were syringe-infiltrated in the abaxial
779 side with bacterial suspensions of *A. citrulli* strains containing 10^8 colony forming units
780 (cfu)/mL in 10 mM $MgCl_2$. Phenotypes were recorded 3 and 4 days after inoculation
781 (d.a.i.), for melon and pepper leaves, respectively. For a better visualization of HR
782 symptoms in pepper leaves, the infiltrated leaves were soaked in an acetic
783 acid:glycerol:water solution (1:1:1 v/v) for 4 h and then transferred to ethanol and
784 boiled for 10 min. Experiments were repeated twice with similar results.
785
786 **RNA isolation, cDNA synthesis and reverse transcription-PCR (RT-PCR)**
787 *Acidovorax citrulli* M6 and *hrpX* mutant were grown at 28 °C in 5 mL of XVM2
788 medium for 72 h. Total RNA was isolated using TRI reagent (Sigma-Aldrich) and
789 Direct-zol RNA miniprep kit (Zymo Research, Irvine, CA, USA) according to
790 manufacturer's instructions. Samples were treated with RNase free DNase using Turbo
791 DNA-free kit (Invitrogen, Carlsbad, CA, USA). RNA concentration was quantified
792 using a Nanodrop DS-11 FX (Denovix, Wilmington, Delaware) and RNA integrity was
793 assayed on 1% agarose gels. RNA was reverse transcribed into cDNA using a High
794 Capacity cDNA Reverse Transcription Kit (Applied Biosystems). Semiquantitative RT-
795 PCR analysis was performed using 1 µg of cDNA or gDNA (as positive control for
796 amplification), 0.6 pmol of selected primer, the Phusion High-Fidelity DNA Polymerase
797 (ThermoFisher Scientific, Waltham, MA, USA), and the following conditions: 98 ºC for
798 15 min, followed by 35 cycles of 98 ºC for 30 s, 60 ºC for 30 s and 72 ºC for 15 s. The
799 *A. citrulli GADPH* housekeeping gene [68] was used as reference. The relative amount
800 of amplified DNA was assayed on 2% agarose gels.

801

802 **RNA-Seq and quality analysis**

803 Total RNA of wild-type M6 and *hrpX* mutant strains was isolated as described
804 above for RT-PCR experiments. Three independent RNA extractions were obtained for
805 each strain. Ribosomal RNA was depleted using the MICROB Express Bacterial
806 mRNA Purification kit (Ambion, Foster City, CA, USA). The integrity and quality of
807 the ribosomal depleted RNA was checked by an Agilent 2100 Bioanalyzer chip-based
808 capillary electrophoresis machine (Agilent Technologies, Santa Clara, CA, USA). RNA
809 sequencing was carried out at the Center for Genomic Technologies at The Hebrew
810 University of Jerusalem (Jerusalem, Israel). The samples were used to generate whole
811 transcriptome libraries using the NextSeq 500 high output kit (Illumina, San Diego, CA,
812 USA) with a NextSeq 2000 sequencing instrument (Illumina). The cDNA libraries were
813 quantified with a Qubit 2.0 Fluorometer (Invitrogen) and their quality was assessed with
814 an Agilent 2200 TapeStation system (Agilent Technologies). One of the *hrpX* mutant
815 libraries was removed from further analysis due to low quality. Raw reads (fastq files)
816 were further inspected with FastQC v0.11.4 [69]. They were trimmed for quality and
817 adaptor removal using Trim Galore default settings: trimming mode, single-end; Trim
818 Galore version 0.4.3; Cutadapt version 1.12; Quality Phred score cutoff, 20; quality
819 encoding type selected, ASCII+33; adapter sequence, AGATCGGAAGAGC (Illumina
820 TruSeq, Sanger iPCR; auto-detected); maximum trimming error rate; 0.1; minimum
821 required adapter overlap (stringency), 1 bp. An average of 0.6% of the reads were
822 quality trimmed and 57% of the reads were treated for adaptor removal.

823

824 **Mapping of RNA-Seq reads on the *A. citrulli* M6 genome and differential**
825 **expression analysis**

826 Cleaned reads (~20 million per sample) were mapped against the latest version
827 of the *A. citrulli* M6 genome (CP029373) using STAR v 2.201 [70]. Mapping files were
828 further processed for visualization by Samtools Utilities v 0.1.19 [71]. The resulting
829 Bam files were used to improve gene and operon predictions along the genome using
830 cufflinks v2.2.1 followed by cuffmerge without a guiding reference file [72]. Uniquely
831 mapped reads per gene were counted twice [once using the original submitted
832 annotation file (orig.gff), and then using the merged annotations by cufflinks-cuffmerge
833 (merged.gff)] using HTSeq-count [73]. Differential expression analysis was performed
834 using the DESeq2 R package [73]. Differentially expressed genes were defined as those
835 genes with a fold-change higher than 2, and a *P* value lower than 0.05.
836
837 **Validation of RNA-Seq results by quantitative real-time PCR (qRT-PCR)**
838 RNA-seq data were verified by qRT-PCR using specific primers of selected
839 genes (S7 Table). Bacterial growth, RNA isolation and cDNA synthesis were as
840 described above for RT-PCR and RNA-Seq experiments. qRT-PCR reactions were
841 performed in a Light Cycler 480 II (Roche, Basel, Switzerland) using 1 μg of cDNA,
842 0.6 pmol of each primer and the HOT FIREPol EvaGreen qPCR Mix Plus (Solis
843 BioDyne, Tartu, Estonia), and the following conditions: 95 ºC for 15 min (1 cycle); 95
844 ºC for 15 s, 60 ºC for 20 s and 72 ºC for 20 s (40 cycles); melting curve profile from 65
845 to 97 ºC to verify the specificity of the reaction. The *A. citrulli GADPH* gene was used
846 as an internal control to normalize gene expression. The threshold cycles (Ct) were
847 determined with the Light Cycler 480 II software (Roche) and the fold-changes of three
848 biological samples with three technical replicates per treatment were obtained by the
849 ΔΔCt method [74]. Significant differences in expression values were evaluated using
850 the Mann-Whitney non-parametrical test ($\alpha = 5\%$).

Additional bioinformatics tools

BlastP analyses for search of T3E homologs were done at the NCBI server against the non-redundant protein sequences (nr) database, selecting the organisms *Acidovorax* (taxid: 12916), *Xanthomonas* (taxid: 338), *Ralstonia* (taxid: 48736) or *Pseudomonas syringae* group (taxid: 136849), with default parameters. Gene ontology (GO) assignments were done using Blast2GO software v5.2 (https://www.blast2go.com/). SignalP4.1 [75], Phobious [76] and Pred-Tat [77] were used for detection of N-terminal type II secretion signal peptides. The program fuzznuc (EMBOSS package; http://www.bioinformatics.nl/cgi-bin/emboss/fuzznuc) was used to detect perfect PIP box sequences (TTCGB-N15-TTCGB; [32]) in the *A. citrulli* M6 genome. A logo of the PIP box motif of *A. citrulli* M6 was done with MEME-ChiP [78] at the MEME Suite website (http://meme-suite.org/). Domain search of T3Es was carried out using the following databases/tools: Protein Data Bank (PDB) and UniProtKB/Swiss-Prot (through NCBI Blast), PFAM (https://pfam.xfam.org/), Prosite (https://prosite.expasy.org/) and InterPro (https://www.ebi.ac.uk/interpro/search/sequence-search). LogSidDB [79] and Plant-mPLoc [80] were used for detection of protein localization signals and for prediction of subcellular localization of T3Es, respectively.

Translocation assays

The ORFs without the stop codon of candidate genes were amplified using specific primers (S7 Table) and cloned into the *Sal*I/*Xba*I sites of pBBR1MCS-2*::avrBs2*$_{62\text{-}574}$, upstream to and in frame with the *avrBs2*$_{62\text{-}574}$ HR domain of *avrBs2* and an haemagglutinin (HA) tag [28], except for ORFs of genes *APS58_0500* and

APS58_1760, which were cloned into the *Xho*I/*Xba*I sites of the same vector. The resulting plasmids were mobilized into *X. euvesicatoria* strains 85-10 *hrpG*ΔavrBs2* [81] and 85-10 *hrpG*ΔhrpF* [82]. Expression of recombinant T3E/CT3E-AvrBs2$_{62\text{-}574}$-HA proteins was verified by Western blot using the iBlot Gel Transfer Stacks Nitrocellulose kit (Invitrogen), and anti- hemagglutinin (HA)-tag and horseradish peroxidase (HRP) antibodies (Cell Signaling Technology, Danvers, MA, USA) (S6 Fig). For translocation assays, *X. euvesicatoria* strains were grown overnight in LB broth with Km, centrifuged and resuspended in 10 mM $MgCl_2$ to a concentration of 10^8 cfu/mL. These suspensions were used to infiltrate the three youngest, fully expanded leaves of 5-week-old ECW20R and ECW30R [83] pepper plants, carrying and lacking the *Bs2* gene, respectively, using a needleless syringe. The plants were kept in a growth chamber at 25 °C, ~50% relative humidity, 12 h day/12 h night. HR was monitored 36 h after inoculation (h.a.i.). For visualization of cell death, the infiltrated leaves were treated as described above for pepper leaves infiltrated with *A. citrulli* strains. Each candidate gene was tested in three independent experiments with at least three plants, with similar results being obtained among replicates and experiments.

Agrobacterium-mediated transient expression and confocal imaging

The ORFs of genes *APS58_0500*, *APS58_1448* and *APS58_4116* were amplified with specific primers (S7 Table) and cloned into pEarlyGate101 binary vector [84], upstream of a Yellow Fluorescence Protein (YFP) encoding gene and an HA tag using the Gateway cloning system (ThermoFisher Scientific). The resulting plasmids were verified by sequencing and mobilized into *A. tumefaciens* GV3101 as indicated above. Transient expression experiments were performed following the protocol described by Roden *et al.* [81] with few modifications. Briefly, overnight cultures of *A. tumefaciens*

GV3101 carrying the different plasmids were centrifuged, and pellets were resuspended in induction solution containing 10 mM $MgCl_2$, 10 mM 2-(N-morpholino)-ethanesulfonic acid (MES), and 200 mM acetosyringone (pH 5.6). The suspensions were incubated at 25 ºC without shaking for 3 h. Bacterial cultures were then diluted to OD_{600nm}~0.6 and infiltrated with a needleless syringe into leaves of 4-week-old *N. benthamiana* plants [85] that were grown in a growth chamber (16 h/26 °C in the light, 8 h/18 °C in the dark; relative humidity set to 70%). Subcellular localization of tested T3Es coupled to YFP were investigated by co-infiltration with *A. tumefaciens* GV3101 carrying monomeric Red Fluorescence Protein fused in frame with the endoplasmid reticulum (ER) marker HDEL (mRFP-HDEL; [86, 87]), the membrane associated SlDRP2A (L. Pizarro and M. Bar, unpublished results) fused to monomeric Cherry fluorescent protein, and by staining with 1 mg/mL 4′,6-diamidino-2-phenylindole (DAPI), that was used to detect the nucleus of the plant cells [88]. As controls, plants were infiltrated with *A. tumefaciens* GV3101 carrying pEarlyGate104 (YFP-encoding gene). Infiltrated plants were kept in the growth chamber at similar conditions as above, and 48 h.a.i., functional fluorophores were visualized using a SPE (Leica Microsystems, Wetzlar, Germany) or a LSM 780 (Zeiss, Oberkochen, Germany) confocal microscope. Images were acquired using two tracks: track 1 for YFP detection, exciting at 514 nm and collecting emission from the emission range 530-560 nm; track 2 for RFP and mCherry detection, exciting at 561 nm and collecting from the emission range 588-641 nm. Images of 8 bits and 1024X1024 pixels were acquired using a pixel dwell time of 1.27, pixel averaging of 4 and pinhole of 1 airy unit. Analysis of colocalization was conducted with Fiji-ImageJ using the Coloc2 tool. For calculating the Pearson correlation coefficient, 15-18 images were analysed. Signal profiles were analysed using the Plot Profile tool [89].

Acknowledgements

We thank Dr. Einat Zelinger from the Interdepartmental Core Facility of the Robert H. Smith Faculty of Agriculture, Food and Environment Hebrew University Interdepartmental Core Facility for her assistance with confocal microscopy. We also thank Dr. Inbar Plaschkes from the Bioinformatics Unit of the Hebrew University of Jerusalem for her assistance with the RNA-Seq data.

References

1. Rosenberg T, Eckshtain-Levi N, Burdman S. Plant pathogenic *Acidovorax* species. In: Murillo J, Jackson R, Vinatzer B, Arnold D, editors. Bacterial-plant interactions: advanced research and future trends. Poole: Caister Academic Press; 2015. pp 83-99.

2. Burdman S, Walcott R. Plant-pathogenic *Acidovorax* species. Saint Paul: American Phytopathological Society; 2018

3. Burdman S, Walcott R. *Acidovorax citrulli*: generating basic and applied knowledge to tackle a global threat to the cucurbit industry. Mol Plant Pathol. 2012; 13:805-815.

4. Zhao M, Walcott R. *Acidovorax citrulli*: History, epidemiology, and management of bacterial fruit blotch of cucurbits. In: Burdman S, Walcott R., editors. Plant-pathogenic *Acidovorax* species. Saint Paul: American Phytopathological Society; 2018. pp. 39-57.

5. Burdman S, Kots N, Kritzman G, Kopelowitz, J. Molecular, physiological, and host-range characterization of *Acidovorax avenae* subsp. *citrulli* isolates from watermelon and melon in Israel. Plant Dis. 2005; 89:1339-1347.

951 **6.** Walcott RR, Fessehaie A, Castro AC. Differences in pathogenicity between two
952 genetically distinct groups of *Acidovorax avenae* subsp. *citrulli* on cucurbit hosts. J
953 Phytopathol. 2004; 152:277-285.
954 **7.** Walcott RR, Langston JDB, Sanders FH, Gitaitis RD. Investigating intraspecific
955 variation of *Acidovorax avenae* subsp. *citrulli* using DNA fingerprinting and whole
956 cell fatty acid analysis. Phytopathology. 2000; 90:191-196.
957 **8.** Eckshtain-Levi N, Shkedy D, Gershovitz M, da Silva GM, Tamir-Ariel D, Walcott
958 R, et al. Insights from the genome sequence of *Acidovorax citrulli* M6, a group I
959 strain of the causal agent of bacterial fruit blotch of cucurbits. Front Microbiol.
960 2016; 7:430.
961 **9.** Yang R, Santos-Garcia D, Pérez-Montaño F, da Silva GM, Zhao M, Jiménez-
962 Guerrero I, et al. Complete assembly of the genome of an A*cidovorax citrulli* strain
963 reveals a naturally occurring plasmid in this species. *Front Microbiol*. Forthcoming
964 (doi: 10.3389/fmicb.2019.01400).
965 **10.** Bahar O, Burdman S. Bacterial fruit blotch: a threat to the cucurbit industry. Israel J
966 Plant Sci. 2010; 58:19-31.
967 **11.** Block A, Li GY, Fu ZQ, Alfano JR. Phytopathogen type III effector weaponry and
968 their plant targets. Curr Opin Plant Biol. 2008; 11:396-403.
969 **12.** Büttner D. Behind the lines-actions of bacterial type III effector proteins in plant
970 cells. FEMS Microbiol Rev. 2016; 40:894-937.
971 **13.** Galan JE, Lara-Tejero M, Marlovits TC, Wagner S. Bacterial type III secretion
972 systems: specialized nanomachines for protein delivery into target cells. Ann Rev
973 Microbiol. 2014; 68:415-438.
974 **14.** Feng F, Zhou JM. Plant-bacterial pathogen interactions mediated by type III
975 effectors. Curr Opin Plant Biol. 2012; 15:469-476.

976 **15.** Macho AP, Zipfel C. Targeting of plant pattern recognition receptor-triggered
977 immunity by bacterial type-III secretion system effectors. Curr Opin Microbiol.
978 2015; 23: 14-22.
979 **16.** Duxbury Z, Ma Y, Furzer OJ, Huh SU, Cevik V, Jones, JDG, et al. Pathogen
980 perception by NLRs in plants and animals: Parallel worlds. Bioessays. 2016;
981 38:769-781.
982 **17.** Jones JD, Dangl JL. The plant immune system. Nature. 2006; 444:323-329.
983 **18.** Flor HH. Current status of the gene-for-gene concept. Ann Rev Phytopathol. 1971;
984 9:275-296.
985 **19.** Bogdanove AJ, Beer SV, Bonas U, Boucher CA, Collmer A, Coplin DL, et al.
986 Unified nomenclature for broadly conserved *hrp* genes of phytopathogenic bacteria.
987 Mol Microbiol. 1996; 20:681-683.
988 **20.** Büttner D, Bonas U. Getting across-bacterial type III effector proteins on their way
989 to the plant cell. EMBO J. 2002; 21:5313-5322.
990 **21.** Büttner D, Bonas U. Regulation and secretion of *Xanthomonas* virulence factors.
991 FEMS Microbiol Rev. 2010; 34:107-133.
992 **22.** Genin S, Denny TP. Pathogenomics of the *Ralstonia solanacearum* species
993 complex. Annu Rev Phythopathol. 2012; 50:67-89.
994 **23.** Wengelnik K, Ackerveken G, Bonas U. HrpG, a key *hrp* regulatory protein of
995 *Xanthomonas campestris* pv. *vesicatoria* is homologous to two-component
996 response regulators. Mol Plant-Microbe Interact. 1996; 196:704-712.
997 **24.** Wengelnik K, Bonas U. HrpXv, an AraC-type regulator, activates expression of
998 five of the six loci in the *hrp* cluster of *Xanthomonas campestris* pv. *vesicatoria*. J
999 Bacteriol. 1996; 178:3462-3469.

1000 **25.** Cunnac S, Boucher C, Genin S. Characterization of the *cis*-acting regulatory
1001 element controlling HrpB-mediated activation of the type III secretion system and
1002 effector genes in *Ralstonia solanacearum*. J Bacteriol. 2004; 186:2309-2318.
1003 **26.** Zhang XX, Zhao M, Yan JP, Yang LL, Yang YW, Guan W., et al. Involvement of
1004 *hrpX* and *hrpG* in the virulence of *Acidovorax citrulli* strain Aac5, causal agent of
1005 bacterial fruit blotch in cucurbits. Front Microbiol. 2018; 9:507.
1006 **27.** Eckshtain-Levi N, Munitz T, Zivanovic M, Traore SM, Sproeer C, Zhao B, et al.
1007 Comparative analysis of type III secreted effector genes reflects divergence of
1008 *Acidovorax citrulli* strains into three distinct lineages. Phytopathology. 2014;
1009 104:1152-1162.
1010 **28.** Teper D, Burstein D, Salomon D, Gershovitz M, Pupko T, Sessa G. Identification
1011 of novel *Xanthomonas euvesicatoria* type III effector proteins by a machine-
1012 learning approach. Mol Plant Pathol. 2016; 17:398-411.
1013 **29.** Nissan G, Gershovits M, Morozov M, Chalupowicz L, Sessa G, Manulis-Sasson S,
1014 et al. Revealing the inventory of type III effectors in *Pantoea agglomerans* gall-
1015 forming pathovars using draft genome sequences and a machine-learning approach.
1016 Mol Plant Pathol. 2018; 19:381-392.
1017 **30.** De Vos P, Willems A, Jones JB. Taxonomy of the *Acidovorax* genus. In: Burdman
1018 S, Walcott R., editors. Plant-pathogenic *Acidovorax* species. Saint Paul: American
1019 Phytopathological Society; 2018. pp. 5-37.
1020 **31.** Wengelnik K, Marie C, Russel M, Bonas U. Expression and localization of HrpA1,
1021 a protein of *Xanthomonas campestris* pv. *vesicatoria* essential for pathogenicity and
1022 induction of the hypersensitive reaction. J Bacteriol.1996; 178:1061-1069.

1023 **32.** Koebnik R, Krüger A, Thieme F, Urban A, Bonas U. Specific binding of the
1024 *Xanthomonas campestris* pv. *vesicatoria* AraC-type transcriptional activator HrpX
1025 to plant-inducible promoter boxes. J Bacteriol. 2006; 188:7652-7660.
1026 **33.** Tai TH, Dahlbeck D, Clark ET, Gajiwala P, Pasion R, Whalen MC, et al.
1027 Expression of the *Bs2* pepper gene confers resistance to bacterial spot disease in
1028 tomato. Proc Natl Acad Sci USA. 1999; 96:14153-14158.
1029 **34.** Roden JA, Belt B, Ross JB, Tachibana T, Vargas J, Mudgett MB. A genetic screen
1030 to isolate type III effectors translocated into pepper cells during *Xanthomonas*
1031 infection. Proc Natl Acad Sci USA. 2004; 101:16624-16629.
1032 **35.** Li R, Liu P, Wan Y, Chen T, Wang Q, Mettbach U, et al. A membrane
1033 microdomain-associated protein, Arabidopsis Flot1, is involved in a clathrin-
1034 independent endocytic pathway and is required for seedling development. Plant
1035 Cell. 2012; 24:2105-2122.
1036 **36.** Alfano JR, Collmer A. Type III secretion system effector proteins: double agents in
1037 bacterial disease and plant disease. Annu Rev Phytopathol 2004; 42:385-414.
1038 **37.** Boller T, He SY. Innate immunity in plants: an arms race between pattern
1039 recognition receptors in plants and effectors in microbial pathogens. Science. 2009;
1040 324:742-744.
1041 **38.** Castiblanco LF, Triplett LR, Sundin GW. Regulation of effector delivery by type
1042 III secretion chaperone proteins in *Erwinia amylovora*. Front Microbiol. 2018;
1043 9:146.
1044 **39.** Kim HS, Thammarat P, Lommel SA, Hogan CS, Charkowski AO. *Pectobacterium*
1045 *carotovorum* elicits plant cell death with DspE/F, but does not suppress callose or
1046 induce expression of plant genes early in plant-microbe interactions. Mol Plant-
1047 Microbe Interact. 2011; 24:773–786.

1048 **40.** Chang JH, Urbach JM, Law TF, Arnold LW, Hu A, Gombar S, et al. A high-
1049 throughput, near-saturating screen for type III effector genes from *Pseudomonas*
1050 *syringae*. Proc Natl Acad Sci USA. 2005; 102:2549-2554.
1051 **41.** Kvitko BH, Park DH, Velasquez AC, Wei CF, Russell AB, Martin GB, et al.
1052 Deletions in the repertoire of *Pseudomonas syringae* pv. *tomato* DC3000 type III
1053 secretion effector genes reveal functional overlap among effectors. PLoS Pathog.
1054 2009; 5:e1000388.
1055 **42.** O'Brien HE, Thakur S and Guttman DS. (2011) Evolution of plant pathogenesis in
1056 *Pseudomonas syringae*: a genomics perspective. Ann Rev Phytopathol. 2011;
1057 49:269-289.
1058 **43.** Schechter LM, Vencato M, Jordan KL, Schneider SE, Schneider DJ, Collmer A.
1059 Multiple approaches to a complete inventory of *Pseudomonas syringae* pv. *tomato*
1060 DC3000 type III secretion system effector proteins. Mol Plant-Microbe Interact.
1061 2006; 19:1180-1192.
1062 **44.** White FF, Potnis N, Jones JB, Koebnik R. The type III effectors of *Xanthomonas*.
1063 Mol Plant Pathol. 2009; 10:749-766.
1064 **45.** Deslandes L, Genin S. (2014) Opening the *Ralstonia solanacearum* type III effector
1065 tool box: insights into host cell subversion mechanisms. Curr Opin Plant Biol.
1066 2014; 20:110-117.
1067 **46.** Peeters N, Carrère S, Anisimova M, Plener L, Cazalé AC, Genin S. Repertoire,
1068 unified nomenclature and evolution of the type III effector gene set in the *Ralstonia*
1069 *solanacearum* species complex. BMC Genomics. 2013; 14:859.
1070 **47.** Guo Y, Figueiredo F, Jones J, Wang N. HrpG and HrpX play global roles in
1071 coordinating different virulent traits of *Xanthomonas axonopodis* pv. *citri*. Mol
1072 Plant-Microbe Interact. 2011; 24:649-661.

1073 **48.** Occhialini A, Cunnac S, Reymond N, Genin S, Boucher C. Genome-wide analysis
1074 of gene expression in *Ralstonia solanacearum* reveals that the *hrpB* gene acts as a
1075 regulatory switch controlling multiple virulence pathways. Mol. Plant-Microbe
1076 Interact. 2005; 18:938-949.
1077 **49.** Valls M, Genin S, Boucher C. Integrated regulation of the type III secretion system
1078 and other virulence determinants in *Ralstonia solanacearum*. PLoS Pathog. 2006;
1079 2:e82.
1080 **50.** Brito B, Marenda M, Barberis P, Boucher C, Genin S. *prhJ* and *hrpG*, two new
1081 components of the plant-signal dependent regulatory cascade controlled by PrhA in
1082 *Ralstonia solanacearum*. Mol Microbiol. 1999; 31:237-251.
1083 **51.** Furutani A, Tsuge S, Ohnishi K, Hikichi Y, Oku T, Tsuno K, et al. Evidence for
1084 HrpXo-dependent expression of type II secretory proteins in *Xanthomonas oryzae*
1085 pv. *oryzae*. J Bacteriol. 2004; 186:1374-1380.
1086 **52.** Szczesny R, Jordan M, Schramm C, Schulz S, Cogez V, Bonas U, et al. Functional
1087 characterization of the Xcs and Xps type II secretion systems from the plant
1088 pathogenic bacterium *Xanthomonas campestris* pv. *vesicatoria*. New Phytol. 2010;
1089 187:983-1002.
1090 **53.** Wang L, Rong W, He C. Two *Xanthomonas* extracellular polygalacturonases,
1091 PghAxc and PghBxc, are regulated by type III secretion regulators HrpX and HrpG
1092 and are required for virulence. Mol Plant-Microbe Interact. 2008; 21:555-563.
1093 **54.** Yamazaki A, Hirata A, Tsuyumu S. HrpG regulates type II secretory proteins in
1094 *Xanthomonas axonopodis* pv. *citri*. J Gen Plant Pathol. 2008; 74:138-150.
1095 **55.** Sambrook J, Fritsch EF, Maniatis T. Molecular cloning: a laboratory manual. Cold
1096 Spring Harbor: Cold Spring Harbor Laboratory; 1989.

1097 **56.** Bahar O, Goffer T, Burdman S. Type IV pili are required for virulence, twitching
1098 motility, and biofilm formation of *Acidovorax avenae* subsp. *citrulli*. Mol Plant-
1099 Microbe Interact. 2009; 22:909-920.
1100 **57.** Zhou H, Morgan RL, Guttman DS, Ma W. Allelic variants of the *Pseudomonas*
1101 *syringae* type III effector HopZ1 are differentially recognized by plant resistance
1102 systems. Mol Plant-Microbe Interact. 2009; 22:176-189.
1103 **58.** Burstein D, Zusman T, Degtyar E, Viner R, Segal G, Pupko T. Genome- scale
1104 identification of *Legionella pneumophila* effectors using a machine learning
1105 approach. PLoS Pathog. 2009; 5:e1000508.
1106 **59.** Lifshitz Z, Burstein D, Schwartz K, Shuman HA, Pupko T, Segal G. Identification
1107 of novel *Coxiella burnetii* Icm/Dot effectors and genetic analysis of their
1108 involvement in modulating a mitogen- activated protein kinase pathway. Infect
1109 Immun. 2014; 82:3740-3752.
1110 **60.** Breiman L. Random forest. Mach Learn. 2001; 45:5-32.
1111 **61.** Langley P, Iba W, Thompson K. An analysis of Bayesian classifiers. In: Aaai- 92,
1112 Proceedings of the tenth national conference on artificial intelligence. San Jose:
1113 AAAI Press; 1992. pp. 223-238.
1114 **62.** Burges CJC. A tutorial on support vector machines for pattern recognition. Data
1115 Min Knowl Discov. 1998; 2:121-167.
1116 **63.** Hastie T, Tibshirani R, Friedman J. The elements of statistical learning. New York:
1117 Springer; 2001
1118 **64.** Pedregosa F, Varoquaux G, Gramfort A, Michel V, Thirion B, Grisel O, et al.
1119 Scikit-learn: machine learning in Python. J Mach Learn Res. 2011; 12:2825-2830.
1120 **65.** Penfold RJ, Pemberton JM. An improved suicide vector for construction of
1121 chromosomal insertion mutations in bacteria. Gene. 1992; 118:145-146.

1122 **66.** Kovach ME, Elzer PH, Hill DS, Robertson GT, Farris MA, Roop RM, et al. Four
1123 new derivatives of the broad-host-range cloning vector pBBR1MCS, carrying
1124 different antibiotic-resistance cassettes. Gene. 1995; 166:175-176.
1125 **67.** Kearney B, Staskawicz BJ. Widespread distribution and fitness contribution of
1126 *Xanthomonas campestris* avirulence gene *avrBs2*. Nature. 1990; 346:385-386.
1127 **68.** Shavit R, Lebendiker M, Pasternak Z, Burdman S, Helman Y. The *vapB-vapC*
1128 operon of *Acidovorax citrulli* functions as a *bona-fide* toxin-antitoxin module. Front
1129 Microbiol. 2016; 6:1499.
1130 **69.** Martin M. Cutadapt removes adapter sequences from high-throughput sequencing
1131 reads. EMBnet J. 2011; 17:10.
1132 **70.** Dobin A, Davis CA, Schlesinger F, Drenkow J, Zaleski C, Jha S, et al. STAR:
1133 ultrafast universal RNA-seq aligner. Bioinformatics. 2013; 29:15-21.
1134 **71.** Li H, Handsaker B, Wysoker A, Fennell T, Ruan J, Homer N, et al. The sequence
1135 alignment/map format and SAMtools. Bioinformatics. 2009; 25:2078-2079.
1136 **72.** Trapnell C, Williams BA, Pertea G, Mortazavi A, Kwan G, Van Baren M, et al.
1137 Transcript assembly and quantification by RNA-Seq reveals unannotated transcripts
1138 and isoform switching during cell differentiation. Nat Biotechnol. 2010; 28:511-
1139 515.
1140 **73.** Anders S, Huber W. Differential expression analysis for sequence count data.
1141 Genome Biol. 2010; 11:R106.
1142 **74.** Pfaffl MW. A new mathematical model for relative quantification in real-time RT-
1143 PCR. Nucleic Acids Res. 2001; 29:e45.
1144 **75.** Petersen N, Brunak S, von Heijne G, Nielsen H. SignalP 4.0: discriminating signal
1145 peptides from transmembrane regions. Nat Methods. 2011; 8:785-786.

1146 **76.** Käll L, Krogh A, Sonnhammer ELL. Advantages of combined transmembrane
1147 topology and signal peptide prediction - the Phobius web server. Nucleic Acids
1148 Res. 2007; 35:W429-432.
1149 **77.** Bagos PG, Nikolaou EP, Liakopoulos TD, Tsirigos KD. Combined prediction of
1150 Tat and Sec signal peptides with Hidden Markov Models. Bioinformatics. 2010;
1151 26:2811-2817.
1152 **78.** Machanick P, Bailey TL. MEME-ChiP: motif analysis of large DNA datasets.
1153 Bioinformatics. 2011; 27:1696-1697.
1154 **79.** Negi S, Pandey S, Srinivasan SM, Mohammed A, Guda C. LogSigDB: a database
1155 of protein localization signals. *Database*. 2015; bav003
1156 (doi:10.1093/database/bav003).
1157 **80.** Chou KC, Shen HB. Cell-PLoc: A package of web-servers for predicting
1158 subcellular localization of proteins in various organisms. Nat Protoc. 2008; 8:135-
1159 162.
1160 **81.** Roden J Eardley L, Hotson A, Cao Y, Mudgett MB. Characterization of the
1161 *Xanthomonas* AvrXv4 effector, a SUMO protease translocated into plant cells.
1162 Mol. Plant-Microbe Interact. 2004; 17:633-643.
1163 **82.** Casper-Lindley C, Dahlbeck D, Clark ET, Staskawicz BJ. Direct biochemical
1164 evidence for type III secretion-dependent translocation of the AvrBs2 effector
1165 protein into plant cells. Proc Natl Acad Sci USA. 2002; 99:8336-8341.
1166 **83.** Minsavage GV, Dahlbeck D, Morales CQ, Whalen MC, Kearny B, Bonas U, et al.
1167 Gene-for-gene reletionships specifying disease resistance in *Xanthomonas*
1168 *campestris* pv. *vesicatoria*-pepper interactions. Mol Plant-Microbe Interact. 1990;
1169 3:41-47.

1170 **84.** Earley KW, Haag JR, Pontes O, Opper K, Juehne T, Song K, et al. Gateway-
1171 compatible vectors for plant functional genomics and proteomics. Plant J. 2006;
1172 45:616-629.
1173 **85.** Goodin MM, Zaitlin D, Naidu RA, Lommel SA. *Nicotiana benthamiana*: its history
1174 and future as a model for plant-pathogen interactions. Mol Plant-Microbe Interact.
1175 2008; 21:1015-1026.
1176 **86.** Runions J, Brach T, Kühner S, Hawes C. Photoactivation of GFP reveals protein
1177 dynamics within the endoplasmic reticulum membrane. J Exp Bot. 2006; 57:43-50.
1178 **87.** Schoberer J, Vavra U, Stadlmann J, Hawes C, Mach L, Steinkellner H, et al.
1179 Arginine/lysine residues in the cytoplasmic tail promote ER export of plant
1180 glycosylation enzymes. Traffic. 2009; 10:101-115.
1181 **88.** Kapuscinski J, Skoczylas B. Simple and rapid fluorimetric method for DNA
1182 microassay. Anal Biochem. 1977; 83:252-257.
1183 **89.** Schindelin J, Arganda-Carreras I, Frise E, Kaynig V, Longair M, Pietzsch T, et al.
1184 Fiji: an open-source platform for biological-image analysis. Nat Methods. 2012;
1185 9:676-682.
1186

1187 ## Supporting information

1188 **S1 Fig. HrpX and HrpG are required for pathogenicity of *Acidovorax citrulli* M6.**
1189 Lesions induced in a melon (cv. HA61428) leaf syringe-infiltrated with 10^8 cfu/mL
1190 suspensions of wild-type M6, but not of M6 mutants defective in *hrpX* and *hrpG* genes.
1191 Partial restoration of the wild-type phenotype was observed following transformation of
1192 the mutants with plasmids pBBR1MCS-5::*hrpX* and pBBR1MCS-5::*hrpG*
1193 (complementation plasmids), respectively. The picture was taken 3 days after
1194 infiltration.

S2 Fig. Subcellular localization of APS_0500. (A) Confocal microscopy images of *N. benthamiana* epidermal cells transiently expressing APS_0500-YFP and different endomembrane compartment markers as indicated. Representative images show APS_0500-YFP (green), the subcellular marker: HDEL-RFP, Free-mCherry or SlDRP2A (magenta) and the superimposed image of both channels (merge). Pearson correlation coefficient of the co-localization between APS_0500-YFP and the markers (N=15-18) was determined using the Coloc2 function from ImageJ. Data represented as mean ± SEM. (B) Confocal microscopy images of *N. benthamiana* epidermal cells transiently expressing the plasma membrane protein Flot1-GFP and Free-mCherry. All the images were acquired 48 h after *A. tumefaciens* infiltration using Zeiss LSM780 (40x/1,2 W Korr). Scale bar 20 µm.

S3 Fig. Subcellular localization of APS_1448. Confocal microscopy images of *N. benthamiana* epidermal cells transiently expressing APS_1448-YFP and different endomembrane compartment markers as indicated. Representative images show APS_1448-YFP (green), the subcellular markers HDEL-RFP, Free-mCherry or SlDRP2A (magenta), and the superimposed image of both channels (merge). Pearson correlation coefficient of the co-localization between APS_1448-YFP and the markers (N=15–18) was determined using the Coloc2 function from ImageJ. Data represented as mean ± SEM. All the images were acquired 48 h after *A. tumefaciens* infiltration using Zeiss LSM780 (40x/1,2 W Korr). Scale bar, 20 µm.

S4 Fig. Subcellular localization of APS_4116. Confocal microscopy images of *N. benthamiana* epidermal cells transiently expressing APS_1448-YFP and different endomembrane compartment markers as indicated. Representative images show APS_1448-YFP (green), the subcellular markers HDEL-RFP, Free-mCherry or SlDRP2A (magenta), and the superimposed image of both channels (merge). Pearson

correlation coefficient of the co-localization between APS_1448-YFP and the markers (N=15–18) was determined using the Coloc2 function from ImageJ. Data represented as mean ± SEM. All the images were acquired 48 h after *A. tumefaciens* infiltration using Zeiss LSM780 (40x/1,2 W Korr). Scale bar, 20 µm.

S5 Fig. Distribution of *Acidovorax citrulli* M6 type III effectors (T3Es) according to their amino acid length. The data are from the annotation (GenBank accession CP029373) of the *A. citrulli* M6 ORFs**.**

S6 Fig. Expression of effector-AvrBs2$_{62-574}$::HA fusion proteins of T3Es that were tested in translocation assays. Total protein was extracted from overnight cultures of *Xanthomonas euvesicatoria* 85-10-*hrpG*-ΔavrBs2* expressing CT3E-AvrBs2$_{62-574}$-HA fusions in plasmid pBBR1MCS-2*::avrBs2*$_{62-574}$. Proteins were analysed by Western blot using HA-tag antibody. XopS (*X. euvesicatoria* effector)-AvrBs2$_{62-574}$::HA was included as positive control. Asterisks indicate the size of the expected bands.

S1 Table. Ranking and prediction scores of open reading frames of *Acidovorax citrulli* AAC00-1 (GenBank accession CP000512.1) in the first machine learning run.

S2 Table. Occurrence of *Acidovorax citrulli* M6 type III effectors in other plant pathogenic *Acidovorax* species.

S3 Table. Differential gene expression as determined by RNA-Seq between *Acidovorax citrulli* M6 and an M6 mutant strain defective in *hrpX* gene, after 72 h of growth in XVM2 minimal medium at 28 °C.

S4 Table. Perfect plant-inducible promoter (PIP) boxes in the *Acidovorax citrulli* M6 genome.

S5 Table. Ranking and prediction scores of open reading frames of *Acidovorax citrulli* M6 (GenBank accession CP029373) in the second machine learning run.

S6 Table. Bacterial strains and plasmids used in this study.

1245 **S7 Table.** DNA oligonucleotide primers used in this study.

1246 **S8 Table.** List and description of the features used for the first and second machine

1247 learning runs.

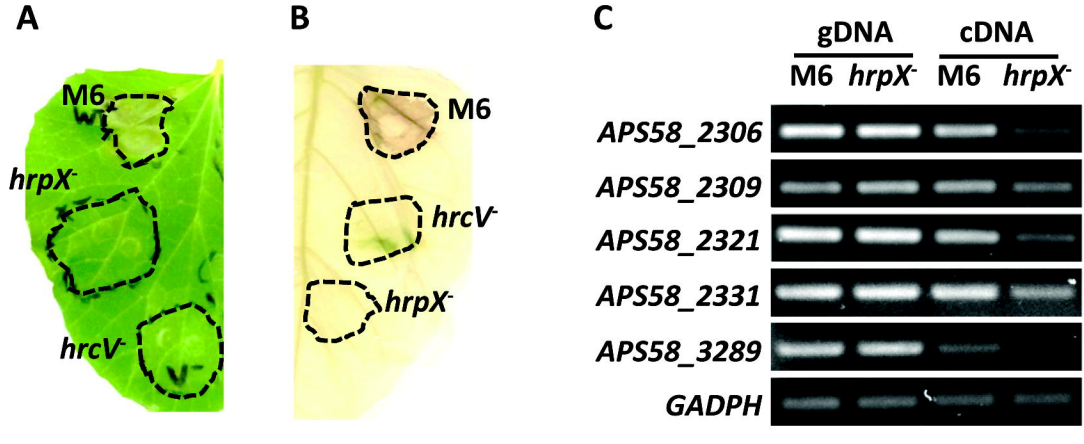
A
M6
hrpX-
hrcV-
B
M6
hrcV-
hrpX-
C
gDNA
cDNA
M6
hrpX-
M6
hrpX-
APS58_2306
APS58_2309
APS58_2321
APS58_2331
APS58_3289
GADPH

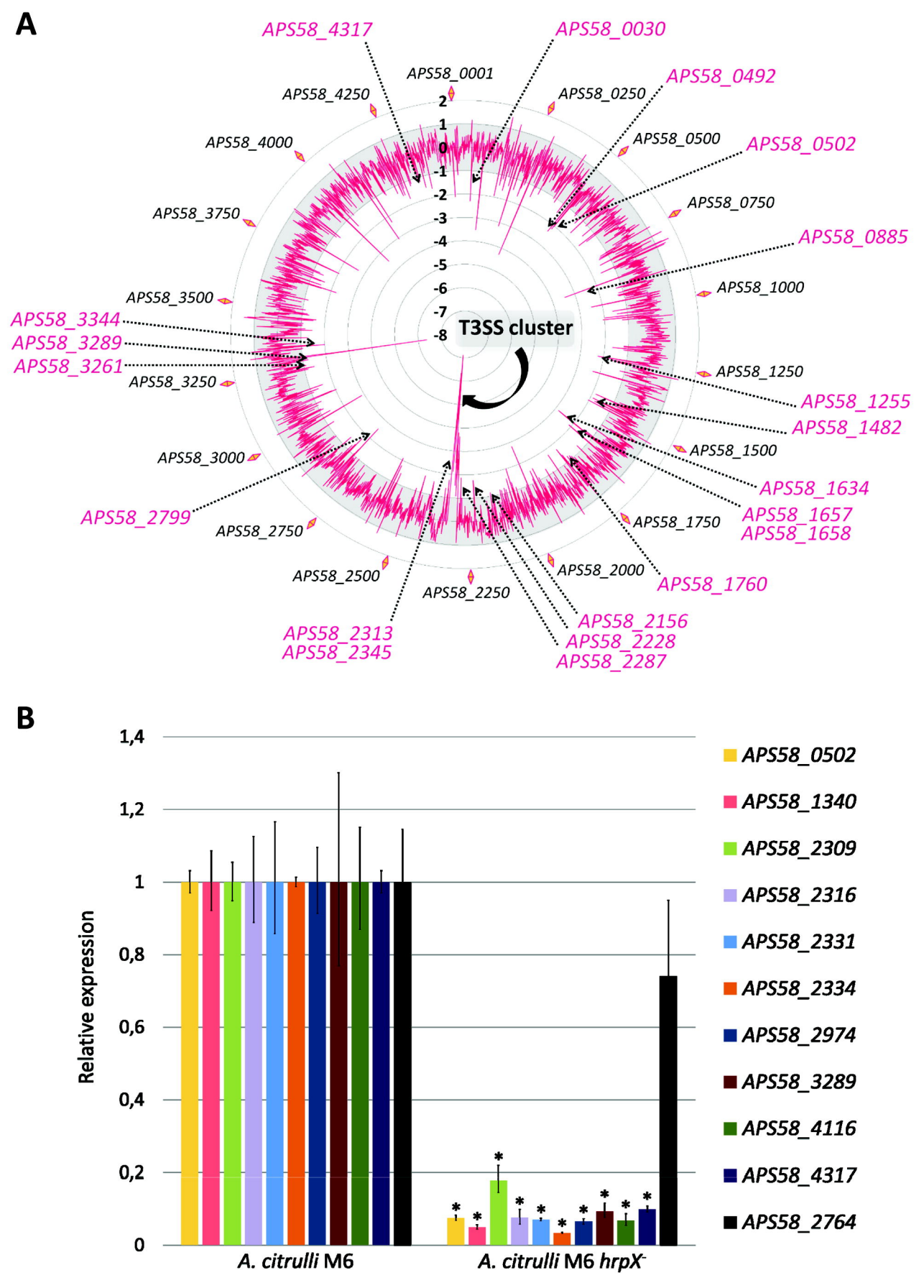
A
APS58_4317
APS58_0030
APS58_0001
APS58_0492
APS58_4250
APS58_0250
APS58_0500
APS58_4000
APS58_0502
APS58_3750
APS58_0750
APS58_0885
APS58_3500
APS58_1000
APS58_3344
APS58_3289
APS58_3261
T3SS cluster
APS58_3250
APS58_1250
APS58_1255
APS58_1482
APS58_3000
APS58_1500
APS58_1634
APS58_2799
APS58_1657
APS58_1658
APS58_2750
APS58_1750
APS58_2500
APS58_2000
APS58_1760
APS58_2250
APS58_2156
APS58_2313
APS58_2345
APS58_2228
APS58_2287
2
1
0
-1
-2
-3
-4
-5
-6
-7
-8
B
Relative expression
1,4
1,2
1
0,8
0,6
0,4
0,2
0
A. citrulli M6
A. citrulli M6 hrpX-
APS58_0502
APS58_1340
APS58_2309
APS58_2316
APS58_2331
APS58_2334
APS58_2974
APS58_3289
APS58_4116
APS58_4317
APS58_2764

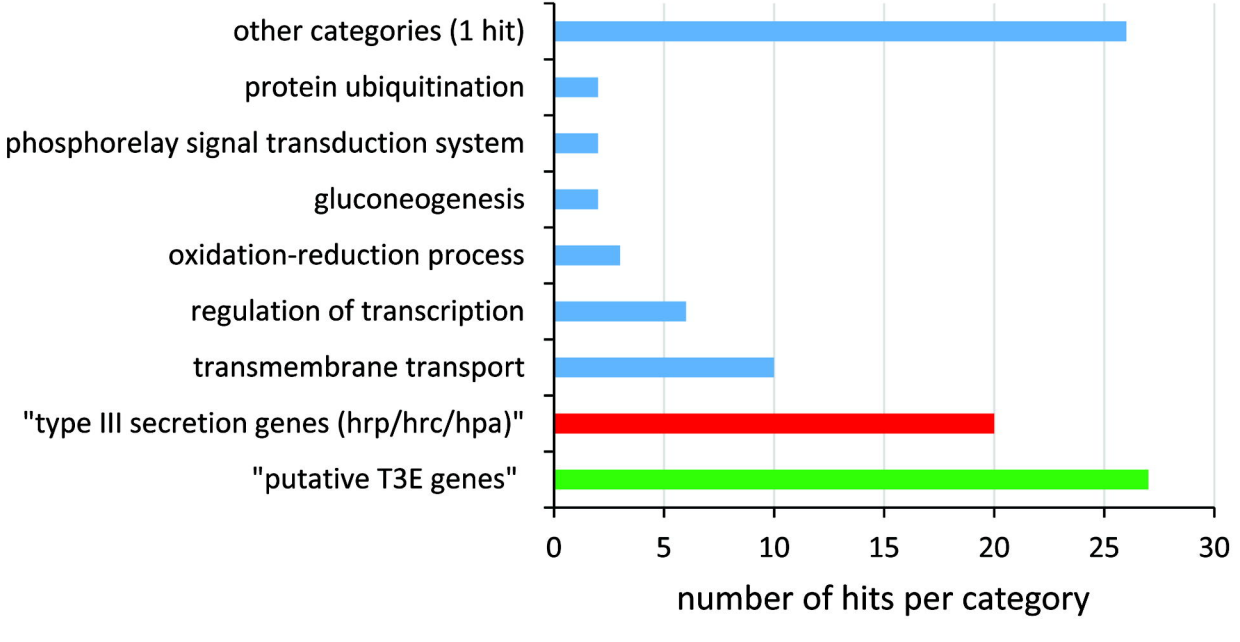
other categories (1 hit)
protein ubiquitination
phosphorelay signal transduction system
gluconeogenesis
oxidation-reduction process
regulation of transcription
transmembrane transport
"type III secretion genes (hrp/hrc/hpa)"
"putative T3E genes"
0
5
10
15
20
25
30
number of hits per category


bits
2
1
0
1
2
3
4
5
6
7
8
9
10
11
12
13
14
15
16
17
18
19
20
21
22
23
24
25

A

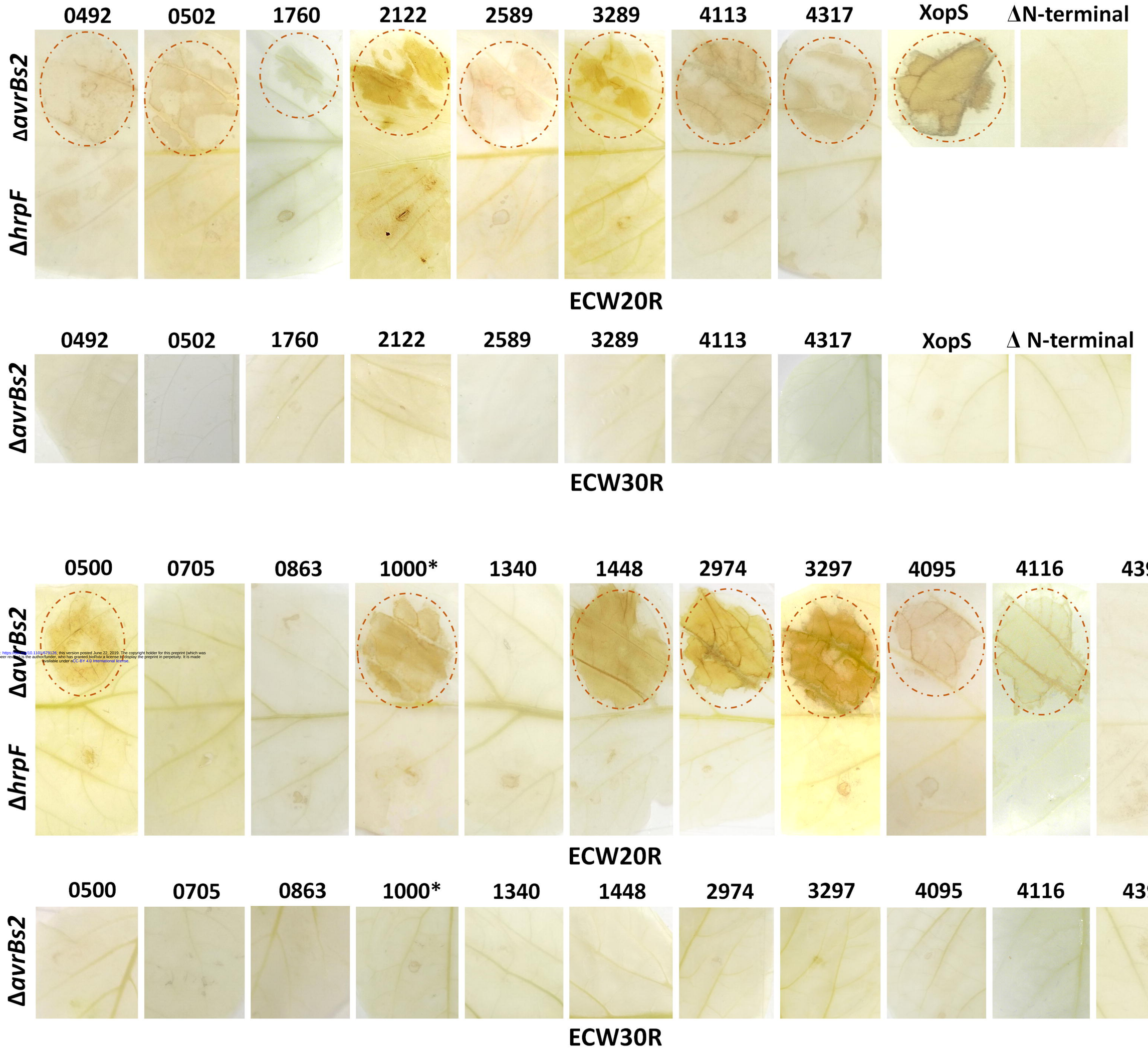

B

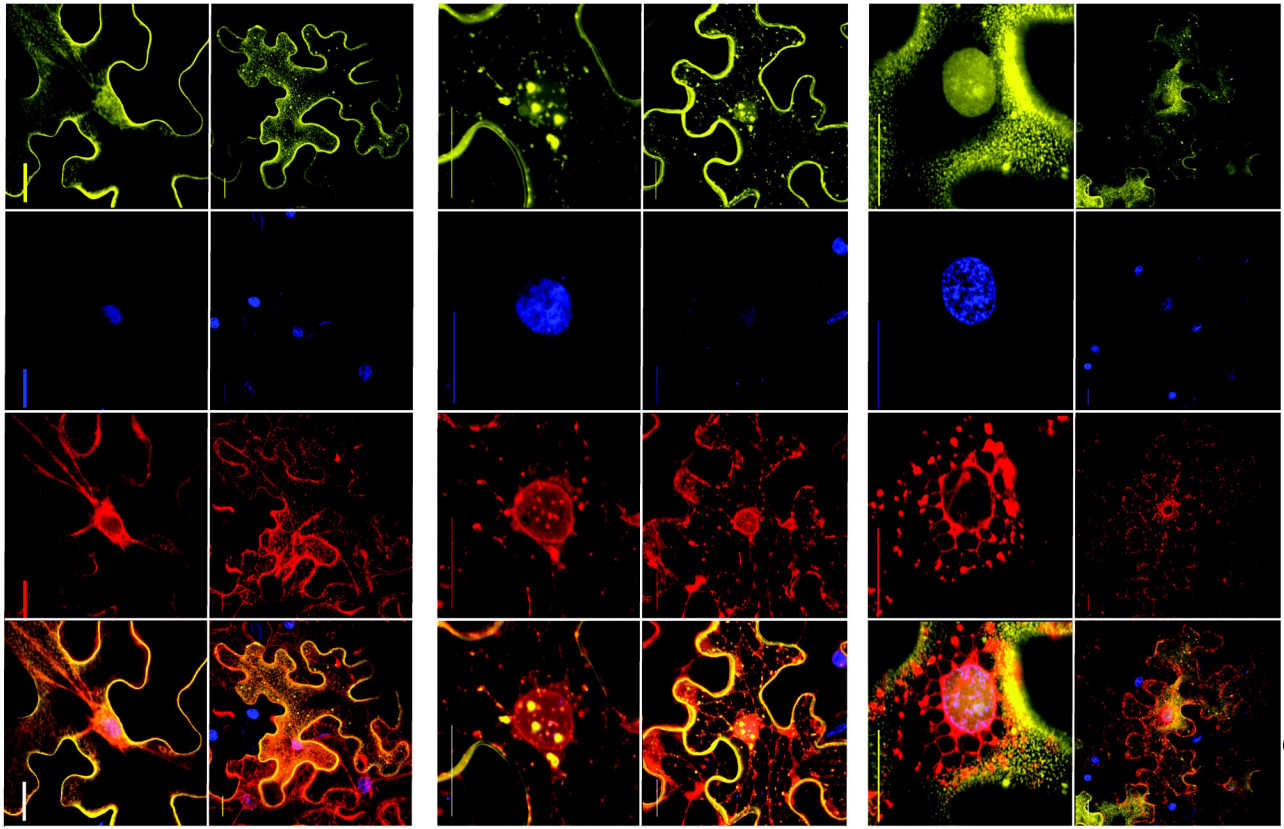
APS58_4116
APS58_1448
APS58_0500
Effector-YFP
DAPI
mRFP-HDEL
merge